https://doi.org/10.5194/egusphere-2026-4549
Preprint. Discussion started: 28 September 2026

Revised nitrogen balance for plant photosynthesis and growth in the dynamic global vegetation, hydrology and agriculture model LPJmL (5.10)

Jens Heinke[1], Sibyll Schaphoff[1], Stephen Björn Wirth[1], and Christoph Müller[1]

[1]Potsdam Institute for Climate Impact Research (PIK), Member of the Leibniz Association, P.O. Box 60 12 03, 14412 Potsdam, Germany

Correspondence: Jens Heinke (heinke@pik-potsdam.de)

Abstract. The balance between the supply of reactive nitrogen to plants and their nitrogen demand determines the extent to which plant growth, and the associated terrestrial carbon and water cycles, are limited by nitrogen (N). While developing recent versions of the Lund-Potsdam-Jena managed land (LPJmL) model, we identified a legacy scaling error in the nitrogen demand formulation that artificially inflated plant leaf N demand by a factor of approximately two. Correcting this structural inconsistency fundamentally altered the modeled terrestrial N balance and effectively eliminated N limitation on simulated vegetation growth. To restore process realism, we present LPJmL version 5.10, which resolves this legacy formulation by implementing a comprehensive re-evaluation of plant uptake, recycling, and phenological dynamics. Specifically, this model update introduces: (1) a corrected leaf N demand calculation that removes inappropriate daylength scaling; (2) updated root uptake kinetics for separate nitrate (NO_3^-) and ammonium (NH_4^+) uptake based on experimental data; (3) changes to N recovery and turnover in plants; and (4) revised tree phenology to improve seasonal canopy dynamics. We evaluated the resulting model behavior using the International Land Model Benchmarking (ILAMB) tool, spatial vegetation patterns against satellite observations, and comparisons with global literature values for N cycle components. LPJmL 5.10 preserves aggregate land-surface performance for energy and hydrological diagnostics while establishing a more self-consistent and realistic internal N cycle. Relative to its predecessor, global vegetation N stocks and N uptake decreased by 35%. This reduction in plant demand shifted mineral soil nitrogen toward a larger nitrate pool, which subsequently increased immobilization, leaching, and denitrification fluxes. These altered pathways bring global N losses into closer agreement with absolute empirical literature estimates. As the final release of the LPJmL 5 series, version 5.10 documents the exact model configuration used for the TRENDY simulations in the Global Carbon Budget 2025 and provides a structurally sound foundation for future model development in the LPJmL 6 series.

https://doi.org/10.5194/egusphere-2026-4549
Preprint. Discussion started: 28 September 2026

1 Introduction

The balance between the supply of reactive nitrogen (Nr) to plants and their nitrogen demand determine the extent to which plant growth and the associated terrestrial carbon and water cycles are limited and controlled by nitrogen (N). At the same time, other growth-regulating mechanisms, such as plant phenology, interact with the seasonal and overall N demand by plants, so that representing the N cycle in models also depends on other mechanisms explicitly and implicitly represented in these. While DGVMs and ESMs have increasingly implemented the N cycle to account for this important control mechanism, the representation of the complexity of the N cycle differs substantially and so do estimates for N stocks and fluxes (Kou-Giesbrecht et al., 2023). Models are often developed over longer time periods, adding additional features (such as an explicit representation of the N dynamics) that may require revisiting existing model components and their parameterization.

The Lund-Potsdam-Jena managed land (LPJmL) model is a dynamic global vegetation, hydrology, and agriculture model originally developed to study the terrestrial carbon cycle of natural and managed ecosystems (Schaphoff et al., 2018b). It was later extended to include the N cycle by von Bloh et al. (2018), including much of the N functionality that was developed for the companion model LPJ-GUESS (Smith et al., 2014). Subsequent model development efforts affecting the representation of the N dynamics include a more explicit representation of biological N fixation (BNF) (Wirth et al., 2024) but also different agricultural management options that affect the N dynamics on managed land (Heinke et al., 2023; Porwollik et al., 2022; Lutz et al., 2019).

When further improving the model, we discovered a bug in the way N demand was computed, which overestimated plant N demand by a factor of approximately two. Correcting that error substantially disturbed the N balance between demand and supply and effectively eliminated N limitation in simulated vegetation growth. Further scrutiny of N uptake, N recycling and plant phenology helped to re-establish a more plausible level of N limitation in LPJmL, version 5.10. These follow-up revisions were developed together as a package, several of them specifically to compensate for the corrected N demand. We therefore present and evaluate them collectively, rather than attributing individual effects to each change. We here describe the changes for documentation and reference and evaluate the resulting model behaviour, making use of the ILAMB (International Land Model Benchmarking) tool, additional variables with substantial changes and a comparison against global literature values for N cycle components. We also discuss two specific limitations that warrant further work: the loosely constrained N uptake kinetics parameters, and the lack of a relationship linking carboxylation capacity back to leaf nitrogen content.

This is the last model update of LPJmL version 5 (von Bloh et al., 2018) before updating to a substantially changed model version (6.0.0, Schaphoff et al., 2026). The LPJmL model version 5.10 was also used for the latest TRENDY simulations for the Global Carbon Budget 2025 (Friedlingstein et al., 2026) and we thus document the final release of the LPJmL 5 series here.

2 Methods

The overall structure and process representation of LPJmL, including vegetation dynamics, phenology, hydrology, crop growth and management, are described in detail by Schaphoff et al. (2018b), and the nitrogen cycle extension of LPJmL5 is documented by von Bloh et al. (2018). In the following, we therefore only summarize those components that have been modified

https://doi.org/10.5194/egusphere-2026-4549
Preprint. Discussion started: 28 September 2026

or newly introduced in LPJmL 5.10, including the coupling between leaf nitrogen and V_{cmax}, the calculation of plant-scale nitrogen demand and uptake, and selected updates to phenology, carbon allocation and management. These targeted descriptions are intended to provide the context needed to understand the model behaviour in this study and to interpret differences relative to previous LPJmL applications.

2.1 Description of the LPJmL model

The Lund-Potsdam-Jena managed land (LPJmL) model is based on the Lund-Potsdam-Jena model (LPJ) that was originally developed for studying vegetation dynamics and the associated carbon cycle under climate change (Sitch et al., 2003) and later extended by hydrological modules (Rost et al., 2008; Gerten et al., 2004) and an representation of agricultural modules for better accounting for human modifications of the terrestrial carbon balance (Bondeau et al., 2007), forming the original LPJmL model that then also represented managed land. Up to version 4 (Schaphoff et al., 2018b, a), biomass stocks and fluxes were only represented as carbon and only climate, atmospheric carbon dioxide concentrations ($[CO_2]$), soil texture, and soil water (managed through irrigation Jägermeyr et al. (2015) and rainwater harvesting Jägermeyr et al. (2016)) determined vegetation patterns and associated carbon stocks in soils and vegetation. The nitrogen cycle was later introduced to the LPJmL model (von Bloh et al., 2018), establishing version 5, in which N availability and plants' demand and uptake capacity effectively limit photosynthesis and growth. Version 5 was the basis for developing different modules for agricultural management (Heinke et al., 2023; Porwollik et al., 2022; Lutz et al., 2019) and further improvements of the core model, including an updated BNF scheme (Wirth et al., 2024).

At the core of the LPJmL model is a photosynthesis module (Haxeltine and Prentice, 1996) that couples the carbon, nitrogen, and water cycles through stomatal exchange with the atmosphere. Assimilated carbon is used to build up biomass in different plant organs (leaves, roots, etc.), which again affects their light interception and subsequent photosynthesis. Natural vegetation is represented as eleven plant functional types (PFTs), of which eight are trees and three are herbaceous. Natural vegetation PFTs compete with each other for resources (light, water, nitrogen) and are assumed to grow in mixed plots. PFTs are parameterized to represent their different life forms (herbaceous vs. trees) and functional types (broadleaved vs. needleleaved, evergreen vs. deciduous) and climatic zones (tropical, temperate, boreal) as well as the corresponding phenology. Vegetation dynamics are represented through establishment, growth, competition, mortality, and wildfires.

Managed vegetation is represented as cropland and managed grasslands. Crops are grown in monocultures, i.e. only one crop at a time, but after harvest, soils of different fields within one grid cell (spatial simulation unit) are mixed to represent rotational management. Crops can be managed differently with tillage (Lutz et al., 2019), irrigation (Jägermeyr et al., 2015), fertilization (von Bloh et al., 2018), manure application (Herzfeld et al., 2021), residue removal (Herzfeld et al., 2021), cover crops (Porwollik et al., 2022), or growing seasons (Minoli et al., 2022). Grasslands are assumed to be perennial grasslands and can be simulated as regularly mowed grassland or with varying livestock densities (Heinke et al., 2023). Land-use patterns, including water reservoirs that can be tapped for irrigation, are prescribed at an annual basis and land pools (soil water, carbon, nitrogen) are adequately transferred across land-use types. Precipitation, irrigation water and snow melt, either infiltrate into the soil column, which is represented in 5 hydrologically active layers (0.2, 0.3, 0.5, 1.0, 1.0 m thick, respectively), where it

https://doi.org/10.5194/egusphere-2026-4549
Preprint. Discussion started: 28 September 2026

percolates through the layers and is available for plant respiration through root uptake, or forms surface runoff. After percolation through the soil column, excess water forms seepage and seepage and runoff are jointly traced through a prescribed river network, from which irrigation water can be extracted (Rost et al., 2008).

A detailed description of the fundamentals of LPJmL is provided by Schaphoff et al. (2018b).

2.2 Updated N processes

2.2.1 Nitrogen demand

Nitrogen of leaves (N_{leaf}) is related to the maximum carboxylation rate of photosynthesis at 25 °C (V_{cmax}^{25}) following Haxeltine and Prentice (1996):

$$N_{leaf} = p \cdot V_{cmax}^{25} + N_0 \; . \tag{1}$$

The parameter p represents the specific leaf nitrogen per unit of V_{cmax}^{25} and is estimated as 0.025 $\mathrm{g(N)\,s\,\mu mol(C)^{-1}}$ based on the regression provided in Field and Mooney (1986). The term N_0 denotes the intercept of the regression and can be interpreted as the structural nitrogen content of leaves. In LPJmL, N_0 is derived from the PFT-specific minimum leaf nitrogen concentration ($NC_{leaf,low}$, in $\mathrm{g(N)\,g(C)^{-1}}$) and the leaf carbon content (C_{leaf}, in $\mathrm{g(C)\,m^{-2}}$) as

$$N_0 = NC_{leaf,low} \cdot C_{leaf} \; . \tag{2}$$

This choice aligns the structural nitrogen requirement in the demand formulation with the minimum leaf C:N ratio that constrains leaf stoichiometry in the model (see Section 2.2.2 and Table 2).

V_{cmax}^{25} is calculated from the optimal maximum carboxylation rate V_{cmax} at ambient temperature T using an exponential function with a temperature sensitivity parameter (k_{temp}) of 0.0693 $\mathrm{K^{-1}}$ (Haxeltine and Prentice, 1996):

$$V_{cmax}^{25} = V_{cmax} \cdot \mathrm{e}^{-k_{temp} \cdot (T-25)} \; . \tag{3}$$

V_{cmax} is calculated by the photosynthesis module of LPJmL to maximize daily net photosynthesis rate (Haxeltine and Prentice, 1996; von Bloh et al., 2018; Schaphoff et al., 2018b). It is internally obtained from fluxes in $\mathrm{g(C)\,m^{-2}\,day^{-1}}$ and multiplied by 0.9645 to convert to $\mathrm{\mu mol(C)\,m^{-2}\,s^{-1}}$, assuming an atomic mass of carbon of 12 $\mathrm{g\,mol^{-1}}$.

This implementation differs in three aspects from the previous version of LPJmL (von Bloh et al., 2018):

1. In von Bloh et al. (2018), V_{cmax} entering the nitrogen demand calculation was scaled with $24/\mathit{daylength}$ following Smith et al. (2014), who introduced this scaling to convert a daily average V_{cmax} to an effective 'daytime' value, by analogy to radiation fluxes. However, V_{cmax} is a leaf-level biochemical capacity per unit leaf area and time, not a daily carbon flux, and the impact of daylength and absorbed photosynthetically active radiation on the optimal V_{cmax} is already accounted for in the photosynthesis routine of LPJmL through the daily optimisation of assimilation (Schaphoff et al., 2018b; Haxeltine and Prentice, 1996). The additional $24/\mathit{daylength}$ factor therefore amounts to a misinterpretation of V_{cmax} as a flux quantity and effectively inflates leaf nitrogen demand. Due to the removal of this scaling, N_{leaf} is on average lower by a factor of approximately two compared to von Bloh et al. (2018).

https://doi.org/10.5194/egusphere-2026-4549
Preprint. Discussion started: 28 September 2026

2. The implementation by von Bloh et al. (2018) included a scaling function $f_{LAI}(LAI)$ applied to V_{cmax}, which increases with leaf area index and was originally introduced by Smith et al. (2014) to account for the empirical observation that leaf nitrogen content declines less sharply with canopy depth than intercepted sunlight. While this mismatch between vertical profiles of leaf nitrogen and absorbed irradiance can be explained by gradients in, for example, hydraulic conductivity or the fraction of diffuse radiation (Peltoniemi et al., 2012; De Pury and Farquhar, 1997), it remains inconsistent with the "big-leaf" assumption commonly used for scaling from leaf to canopy (De Pury and Farquhar, 1997). In the big-leaf framework, V_{cmax} represents an effective canopy-average capacity, and introducing an explicit $f_{LAI}(LAI)$ factor on V_{cmax} interacts in a non-transparent way with leaf stoichiometry, light-use efficiency, transpiration, and other processes that depend on aggregating leaf-level properties to the canopy scale. As such, the observed discrepancy highlights structural shortcomings of the big-leaf assumption rather than supporting the notion of a non-optimal nitrogen distribution per se. After careful consideration, we concluded that this issue should be addressed more fundamentally in future work and therefore decided to remove the scaling function in the current implementation.

3. The implementation by von Bloh et al. (2018) used a lower value for k_{temp} of 0.02 K^{-1}, which results in a much weaker temperature dependence of V_{cmax}^{25} and is not consistent with Haxeltine and Prentice (1996) and other studies (e.g. Bernacchi et al., 2001). In the current implementation, we revert to the original value of 0.0693 K^{-1} from Haxeltine and Prentice (1996) and apply this parameter consistently in both the nitrogen demand calculation and the V_{cmax}-limitation routine.

Total plant nitrogen demand N_{demand} is calculated as in von Bloh et al. (2018) from leaf nitrogen demand and the structural nitrogen requirements of roots, sapwood and, for crops, storage organs. Cumulative carbon allocated to each organ since the beginning of the year is multiplied by prescribed organ-specific C:N ratios to obtain the additional nitrogen required for growth, which is then added to the current leaf nitrogen demand derived from V_{cmax}^{25}. When actual plant nitrogen falls short of this demand, the achievable V_{cmax}^{25} is obtained by inverting Eq. (1): V_{cmax}^{25} is scaled proportionally to the non-structural fraction of N_{leaf} (i.e. $N_{leaf} - N_0$) that can actually be supplied, so that N limitation acts directly on photosynthetic capacity. In LPJmL 5.10 this allocation-based scheme is unchanged; only the leaf nitrogen demand is updated according to the revised N_{leaf}–V_{cmax}^{25} relationship described above.

2.2.2 Nitrogen uptake

Nitrogen uptake in LPJmL 5.10 follows the root uptake concept of Smith et al. (2014) as implemented in LPJmL5 by von Bloh et al. (2018), but is extended to treat nitrate (NO_3^-) and ammonium (NH_4^+) separately with substrate-specific uptake kinetics.

For each soil layer l, substrate-specific potential uptake rates $V_l^{NO_3^-}$ and $V_l^{NH_4^+}$ in $\mathrm{g(N)\,g(C)^{-1}\,d^{-1}}$ are first calculated by a Michaelis–Menten-type saturation function:

$$V_l^{\mathrm{NO_3^-}} = V_{\max}^{\mathrm{NO_3^-}} \cdot \left(k_{\min}^{\mathrm{NO_3^-}} + \frac{\mathrm{NO_{3,l}^-}}{\mathrm{NO_{3,l}^-} + K_m^{\mathrm{NO_3^-}} \cdot \theta_{\max,l} \cdot d_l} \right), \tag{4}$$

https://doi.org/10.5194/egusphere-2026-4549
Preprint. Discussion started: 28 September 2026

and analogously for ammonium,

$$V_l^{\mathrm{NH_4^+}} = V_{\max}^{\mathrm{NH_4^+}} \cdot \left(k_{\min}^{\mathrm{NH_4^+}} + \frac{\mathrm{NH}_{4,l}^+}{\mathrm{NH}_{4,l}^+ + K_m^{\mathrm{NH_4^+}} \cdot \theta_{\max,l} \cdot d_l} \right) . \tag{5}$$

Where $\mathrm{NO}_{3,l}^-$ and $\mathrm{NH}_{4,l}^+$ are the amounts (or concentrations) of nitrate and ammonium in soil layer l in $\mathrm{g(N)\,m^{-2}}$, $\theta_{\max,l}$ is the fractional pore space, and d_l is the thickness of soil layer l in m. $V_{\max}^{\mathrm{NO_3^-}}$ and $V_{\max}^{\mathrm{NH_4^+}}$ are the maximum uptake capacities per unit root carbon for nitrate and ammonium, and $K_m^{\mathrm{NO_3^-}}$ and $K_m^{\mathrm{NH_4^+}}$ are half-saturation parameters for the respective substrates, $k_{\min}^{\mathrm{NO_3^-}}$ and $k_{\min}^{\mathrm{NH_4^+}}$ are dimensionless basal uptake coefficients not associated with Michaelis–Menten kinetics. Estimates for these parameters are summarized in Table 1.

Table 1. Root nitrogen uptake parameters. Values from Craig et al. (2025) represent the sample median adapted to match LPJmL units and conventions. $k_{\min}$ is retained from Zaehle et al. (2010), as Craig et al. (2025) does not constrain this term.

Parameter	Description	$\mathrm{NO_3^-}$	$\mathrm{NH_4^+}$	Units	Source
$V_{\max}$	Maximum uptake capacity per unit root carbon	1.5×10^{-3}	4.7×10^{-3}	$\mathrm{g(N)\,g(C)^{-1}\,d^{-1}}$	Craig et al. (2025)
K_m	Half-saturation concentration	0.70	0.45	$\mathrm{g(N)\,m^{-3}}$	Craig et al. (2025)
$k_{\min}$	Non–Michaelis–Menten uptake rate fraction	0.05	0.05	–	Zaehle et al. (2010)

Total mineral nitrogen uptake is then obtained as

$$\mathrm{N_{uptake}} = \sum_{l=1}^{n_{\mathrm{soillayer}}} \left(V_l^{\mathrm{NO_3^-}} + V_l^{\mathrm{NH_4^+}} \right) \cdot \mathrm{C_{root},}_l \cdot f_T(T_{\mathrm{soil},l}) \cdot f_{\mathrm{NC}}(\mathrm{NC_{plant}}) , \tag{6}$$

where $n_{\mathrm{soillayer}}$ is the number of soil layers, $\mathrm{C_{root},}_l$ is root carbon in layer l in $\mathrm{g(C)\,m^{-2}}$, $T_{\mathrm{soil},l}$ is soil temperature, and $\mathrm{NC_{plant}}$ is the whole-plant nitrogen-to-carbon ratio. The function $f_T(T_{\mathrm{soil},l})$ describes the dependence of uptake on soil temperature and remains the same as in the original LPJmL5 implementation by von Bloh et al. (2018) following Thornley (1991):

$$f_T(T_{\mathrm{soil},l}) = \max\left(0, \frac{(T_{\mathrm{soil},l} - T_0)\,(2T_m - T_0 - T_{\mathrm{soil},l})}{(T_r - T_0)\,(2T_m - T_0 - T_r)}\right) . \tag{7}$$

For the parameterisation $T_0 = -25$ °C, $T_r = 15$ °C, and $T_m = 15$ °C used in LPJmL5, the function is zero below -25 °C, increases to unity at 15 °C, and declines again towards zero at higher temperatures (reaching zero at 55 °C).

The function $f_{\mathrm{NC}}(\mathrm{NC_{plant}})$ describes the dependence of uptake on plant nitrogen status, and retains the same role as in the original LPJmL5 implementation. However, its formulation has been changed from the version of Zaehle et al. (2010) used in the original LPJmL5 implementation to the formulation given by Smith et al. (2014):

$$f(NC_{\mathrm{plant}}) = \min\left(1, \max\left(0, \frac{\mathrm{NC_{plant}} - 1/\mathrm{CN_{leaf,low}}}{\frac{2}{\mathrm{CN_{leaf,high}} + \mathrm{CN_{leaf,low}}} - 1/\mathrm{CN_{leaf,low}}}\right)\right) , \tag{8}$$

https://doi.org/10.5194/egusphere-2026-4549
Preprint. Discussion started: 28 September 2026

where $CN_{leaf,high}$ and $CN_{leaf,low}$ are the PFT-specific maximum and minimum leaf C:N ratios, respectively. We use newly derived PFT-specific estimates for $CN_{leaf,low}$ and $CN_{leaf,high}$ based on TRY leaf C:N ranges (Table 2), which are also used consistently in the nitrogen demand formulation. Unlike in the original LPJmL5 implementation, which reaches unity only at $CN_{leaf,high}$, this formulation results in $f(NC_{plant}) = 1$ when the whole-plant N:C ratio reaches the midpoint between the minimum and maximum leaf C:N ratios, i.e. when leaf C:N is halfway between its prescribed limits.

Table 2. Natural PFT CN_{leaf} ranges derived from TRY database (Kattge et al., 2011) and $f_{N,turnover}$ informed by Sophia et al. (2024).

PFT	$CN_{leaf,low}$	$CN_{leaf,med}$	$CN_{leaf,high}$	$f_{N,turnover}$
Tropical broadleaved evergreen tree	14.8	24.8	41.6	0.50
Tropical broadleaved raingreen tree	13.5	22.1	32.8	0.50
Temperate needleleaved evergreen tree	28.9	43.4	65.1	0.70
Temperate broadleaved evergreen tree	14.8	24.8	41.6	0.30
Temperate broadleaved summergreen tree	13.5	22.1	32.8	0.30
Boreal needleleaved evergreen tree	28.9	43.4	65.1	0.70
Boreal broadleaved summergreen tree	13.5	22.1	32.8	0.30
Boreal needleleaved summergreen tree	18.6	26.0	36.3	0.30
Tropical C4 grass	13.1	28.4	61.2	0.35
Temperate C3 grass	9.9	24.8	41.6	0.35
Polar C3 grass	9.9	24.8	41.6	0.28
Bioenergy tropical tree	14.8	24.8	41.6	0.48
Bioenergy temperate tree	13.5	22.1	32.8	0.37
Bioenergy C4 grass	34.0	90.0	132.0	0.69
Crops	14.3	25.0	58.8	0.30

2.2.3 Nitrogen turnover and recovery in plants

LPJmL applies daily turnover rates for plant tissues such that, over the course of a year, they match a PFT-specific annual turnover rate for each tissue type. While all carbon associated with tissue turnover enters the litter pool, only part of the nitrogen associated with tissue turnover is lost to litter; the remainder is recovered by the plant. In the original LPJmL5 implementation, this recovered N was not made available to the plant immediately, but only accounted for during annual bookkeeping at the end of each year. In LPJmL5.10, the recovered N is instead added directly to the biomass increment N pool and enters the daily N budget. This daily allocation of recovered N directly increases nitrogen content of plant tissues and can relax N limitation on growth and photosynthesis.

The revised handling of N recovery is accompanied by an updated parameterisation of the recoverable fraction of leaf N at turnover. For each PFT, the parameter $f_{N,turnover}$ defines the fraction of senescent leaf N that is irreversibly lost to litter; the remainder is assumed to be translocated before leaf shedding. We re-parameterized $f_{N,turnover}$ against the global synthesis

https://doi.org/10.5194/egusphere-2026-4549
Preprint. Discussion started: 28 September 2026

of leaf N resorption efficiencies compiled by Sophia et al. (2024), assigning the same $f_{N,\text{turnover}}$ to both tropical tree PFTs, reducing the value for needleleaved PFTs, and increasing the value for grass PFTs (Table 2). However, we retain low $f_{N,\text{turnover}}$ for all non-tropical deciduous tree PFTs to maintain their competitiveness in N-limited ecosystems.

2.3 Tree phenology and other changes

Tree leaf phenology is represented by the scalar variable *phen*, which scales active leaf area between 0 and 1 and is controlled by multiplicative limiting functions for cold- and heat-temperature stress, light availability, and soil water availability, following the growing season index (GSI) approach of Forkel et al. (2014). In the previous implementation, *phen* continued to be recalculated daily from these limiting functions even after leaf shedding, so that favourable conditions could let leaf area grow back within the same phenological cycle – an effect most pronounced for raingreen trees in the inner tropics, where the GSI product remains high year-round. In contrast, LPJmL 5.10 sets *phen* to zero at shedding and holds it there until the next cycle begins: deciduous tree PFTs now reach a true end of the growing season.

For both summergreen and raingreen trees, leaf shedding is triggered as a discrete event when the active phenological period exceeds a prescribed maximum duration, or when *phen* falls below 0.1 after a minimum active period. For summergreen trees, the minimum active period was increased from 60 to 90 days and the maximum active period was reduced from 245 to 180 days. For raingreen trees, shedding is additionally triggered just before the onset of the next rainy season, which also marks the start of the following phenological cycle and is defined as the first month of the six-month period with the highest mean precipitation. Leaves were previously lost only through continuous daily turnover rather than through this discrete event. Tropical evergreen trees are exempted from this cycle altogether and are kept fully leaf-active throughout the year by fixing *phen* at 1.

Additional parameter changes were introduced to restore plausible aggregate model behaviour after the correction to nitrogen demand. Several of these, including the temperature boundary below and α_a and θ, are recalibrations of existing parameters rather than corrections grounded in new data; others, such as $nfixpot$ and the dark-respiration parameter b, are updated based on independent literature estimates. The temperature boundary separating temperate from boreal tree PFTs was shifted from -2°C to -5°C, which affects the climatic domain in which temperate and boreal trees can establish. The potential biological nitrogen fixation rate $nfixpot$ was raised from 0.01 to 0.5, corresponding to the midpoint of the range proposed by Yu and Zhuang (2020a). Leaf and root turnover parameters were set to 2 for temperate needleleaved evergreen trees and 3 for boreal needleleaved evergreen trees. For natural vegetation, α_a (the scaling factor from leaf to ecosystem level) was increased from 0.5 to 0.7 and θ (the co-limitation parameter) from 0.90 to 0.95 (for more information see Schaphoff et al. (2018b)). The parameter b, the ratio of dark respiration R_d to V_max, was set to 0.031 for both C_3 and C_4 plants at 25 °C (Wang et al., 2020), and now acclimates to the mean temperature of the vegetation period following Wang et al. (2020).

https://doi.org/10.5194/egusphere-2026-4549
Preprint. Discussion started: 28 September 2026

3 Model evaluation

For evaluating LPJmL 5.10, we conducted a standard simulation and compared it with a corresponding simulation using the predecessor model version LPJmL 5.9.27 and with observational and observation-derived reference data. The evaluation focuses on whether the bug fix and subsequent process updates preserve the broader behaviour of LPJmL while producing a more coherent internal N cycle. As noted above, these revisions were developed as a single package; we therefore evaluate LPJmL 5.10 as a whole rather than attributing individual effects to specific process updates. Within this evaluation, we distinguish between several levels of evidence: aggregate benchmark skill against observational products (Sect. 3.2), spatial vegetation patterns (Sect. 3.3), crop model performance (Sect. 3.4), global C–N balance components relative to the predecessor version (Sect. 3.5), absolute agreement with published literature estimates (Sect. 3.6), and the transient nitrogen balance (Sect. 3.7).

3.1 Modeling protocol

Each standard simulation consists of a sequence of three simulations: a) a spinup simulation (PNV spinup) with natural vegetation only of 3500 years to bring soil and vegetation pools into a hypothetical, dynamic equilibrium in the absence of anthropogenic disturbances or trends in drivers; b) a land-use spinup (LU spinup), in which land-use patterns are gradually introduced, starting in the year 1481, ending in 1900; c) a transient simulation from 1901 to 2019 with dynamic changes in climate, [CO_2], land-use patterns, and land management.

Climatic data from 1901-1930 are repeatedly used in shuffled form during the two spinup simulations PNV spinup and LU spinup. All other data are read in for the periods for which they are available and the first available value is used for all simulation years before and the last available value is used to all simulation years after the period for which data are available.

The standard simulations were driven with the GSWP3-W5E5 climate data (Lange et al., 2023), a combination of W5E5 v2.0 (Cucchi et al., 2020; Lange et al., 2021) for the period 1979–2019 and GSWP3 v1.09 (Kim, 2017) for the period 1901–1978. GSWP3 data have been bias-adjusted towards W5E5 to reduce discontinuities at the 1978/1979 transition (Mengel et al., 2021). Annual, global [CO_2] values are from the TRENDY project (Friedlingstein et al., 2023). Data on land-use and land management are harmonized from different data sources, making use of the LandInG toolbox (Ostberg et al., 2023). Data processed with LandInG include gridded datasets including cropland and pasture extent from HYDE v3.2.1 (Klein Goldewijk et al., 2017), multiple-cropping suitability from GAEZ v3 (IIASA/FAO, 2012), and crop-specific harvested areas for the year 2000 (Monfreda et al., 2008) as well as census data at national scale from FAOSTAT (FAO, 2020b), AQUASTAT (FAO, 2020a), and MIRCA2000 (Portmann et al., 2010a, b). Crop-specific fertilizer application patterns for the year 2000 (Mueller et al., 2012; Mueller, 2012) are combined with national-scale fertilizer application trends (Hurtt et al., 2020) to derive gridded time series of crop-specific nitrogen fertilizer application rates. Manure application rates (Zhang et al., 2017; Zhang et al., 2017) are assumed to be applied uniformly to all fields within one grid cell. Crop-specific growing periods are based on the GGCMI phase 3 crop calendar (Jägermeyr et al., 2021). On managed grassland livestock densities are prescribed based on Heinke (2025). Soil texture and soil acidity (pH) are assumed static throughout the simulation and values are based on HWSD

https://doi.org/10.5194/egusphere-2026-4549
Preprint. Discussion started: 28 September 2026

v1.21 (FAO/IIASA/ISRIC/ISSCAS/JRC, 2012; Ostberg et al., 2023). The river network is based on STN-30 (Vörösmarty et al., 2000), while lake surface areas are taken from GLWD (Lehner and Döll, 2004). Dam and reservoirs are parameterized based on the GRanD database (Lehner et al., 2011; Biemans et al., 2011). Water use for households, industry and livestock in each grid cell is taken from Flörke et al. (2013, prioritized over irrigation; accounting for 201 km^3 in the year 2000).

3.2 ILAMB benchmark against observational data

We used ILAMB to test whether the process changes in LPJmL 5.10 altered standard land-surface diagnostics relative to LPJmL 5.9.27. The full ILAMB report, including maps, time series, spatial integrals, and score components for each benchmark data set, is provided in the Zenodo archive (Heinke et al., 2026). Here, we summarize the main benchmark scores for the surface energy balance, carbon cycle, and terrestrial hydrology (Table 3).

Across the evaluated variables, LPJmL 5.10 performs similarly to LPJmL 5.9.27, but the response differs among diagnostic groups. The overall scores change only modestly for energy and hydrological diagnostics. For the radiation and energy cycle, albedo improves slightly in the multi-data-set mean (0.586 compared with 0.579), whereas latent heat flux remains nearly unchanged (0.691 compared with 0.696). Hydrological scores are also close to the previous version, although runoff (0.676 compared with 0.681) and evapotranspiration (0.665 compared with 0.687) both decrease slightly.

For carbon-cycle variables, the response is more mixed. Net ecosystem exchange changes little in the overall mean (0.431 compared with 0.430), with improved RMSE and seasonal-cycle scores partly offset by the low spatial-distribution score against FLUXCOM. Gross primary productivity (GPP) shows improved RMSE and seasonal-cycle scores, but its overall mean is slightly lower in LPJmL 5.10 (0.597 compared with 0.611), mainly because of reduced bias scores. Biomass scores decrease moderately in the mean (0.615 compared with 0.639), although LPJmL 5.10 performs slightly better for the tropical and Xu–Saatchi data sets. The largest decline occurs for soil carbon, where the overall mean decreases from 0.446 to 0.383, mainly through lower spatial-distribution scores against both HWSD and NCSCDV22.

ILAMB relationship diagnostics provide an additional test of whether simulated variables covary realistically with climatic drivers (Table 4). These scores also remain broadly similar between the two model versions, but again show no systematic improvement. LPJmL 5.10 slightly improves the GPP–precipitation relationship against FLUXCOM, but relationship scores for biomass and evapotranspiration decrease modestly.

3.3 Vegetation distribution

The spatial comparison of natural vegetation fractions shows that LPJmL 5.10 preserves the main global vegetation gradients simulated by LPJmL 5.9.27, but redistributes cover among tree PFTs in several regions (Fig. 1). Broadleaved evergreen trees remain concentrated in Amazonia, central Africa, and Southeast Asia, consistent with ESA CCI LC4. An important improvement relative to LPJmL 5.9.27 is the reduction of raingreen (broadleaved deciduous) trees in the inner tropics, accompanied by stronger evergreen dominance in the humid rainforest regions; discrepancies remain in the placement of forest–savanna transition zones. Needleleaved evergreen cover remains concentrated in the boreal zone, while needleleaved deciduous cover is mainly simulated over eastern Siberia, broadly matching the observed larch-dominated region but with a smoother and more

https://doi.org/10.5194/egusphere-2026-4549
Preprint. Discussion started: 28 September 2026

extensive distribution than in ESA CCI LC4, and boreal–temperate transitions remain insufficiently sharp. Grass cover changes complement these tree-cover shifts and highlight remaining biases in semi-arid, open vegetation, especially where the model simulates too much tree cover in transition regions.

3.4 Crop model performance

We evaluated crop model performance by comparing interannual yield anomalies from LPJmL 5.9.27 and LPJmL 5.10 against FAOstat national yield statistics and the GGCMI Phase 1 model ensemble (Müller et al., 2017), using the GGCMI crop model evaluation tool. This comparison assesses how well the model captures climate-driven interannual yield variability at the global aggregate scale; absolute yield levels are not evaluated here, as LPJmL is not calibrated to match FAOstat yield levels. The time series for maize, wheat, soybean, and rice are provided in Appendix B (Figs. B1–B4).

Maize shows the strongest agreement with FAOstat in both versions ($r = 0.802$ and $r = 0.825$ for LPJmL 5.10 and 5.9.27, respectively, both $p < 0.001$), broadly competitive with the better-performing members of the GGCMI ensemble. Wheat and soybean show moderate but significant correlations ($r \approx 0.47$, $p < 0.01$), while rice interannual correlations remain non-significant in both versions ($r \approx 0.27$), consistent with the finding of Müller et al. (2017) that rice yield variability cannot be well reproduced by most global gridded crop models. Interannual correlations with FAOstat differ only marginally between the two model versions across all four crops, consistent with the unchanged crop phenology and harvest routines in LPJmL 5.10.

3.5 Benchmark comparison with LPJmL 5.9.27

We compared LPJmL 5.10 with LPJmL 5.9.27 for a set of global carbon, nitrogen, fire, and water-balance variables. The main-text comparison focuses on the transient land-use (LU) simulation because it includes natural vegetation, managed grasslands, cropland, fertilization, manure application, and land-use change (Table 5). The corresponding potential natural vegetation (PNV) comparison is provided in Appendix A; most changes have the same sign as in the LU simulation. Full benchmark PDFs for all compared variables are provided in the Zenodo archive (Heinke et al., 2026).

The largest changes occur in nitrogen variables. Vegetation N decreases by 35% and N uptake by 36%, consistent with the revised, lower N demand for photosynthesis and growth. At the same time, total mineral soil N increases, with a strong shift from NH_4^+ to NO_3^-: soil NH_4^+ decreases by 28%, whereas soil NO_3^- more than doubles. The larger mineral N pool is associated with higher immobilization, leaching, and denitrification losses, while mineralization decreases by 8%. N volatilization changes little in the LU simulation, and BNF remains almost unchanged.

Despite lower N uptake, GPP and net primary production (NPP) increase by about 7–8%, indicating that the reduction in plant N demand more than offsets the lower simulated uptake. GPP increases by about 7%, but since autotrophic and heterotrophic respiration increase proportionally less, NPP and net ecosystem production (NEP = NPP − heterotrophic respiration) show progressively larger relative gains of about 8 and 9%, respectively. Harvest C is nearly unchanged between versions, and the 13% increase in fire C emissions amounts to only 0.25 GtC yr^{-1} in absolute terms, so the NEP gain is only marginally reduced. The resulting net biome production (NBP) increase of 0.44 GtC yr^{-1} is therefore large in relative terms (54%), reflecting NBP's small absolute baseline. Vegetation C decreases slightly, whereas soil C and soil N increase. The

https://doi.org/10.5194/egusphere-2026-4549
Preprint. Discussion started: 28 September 2026

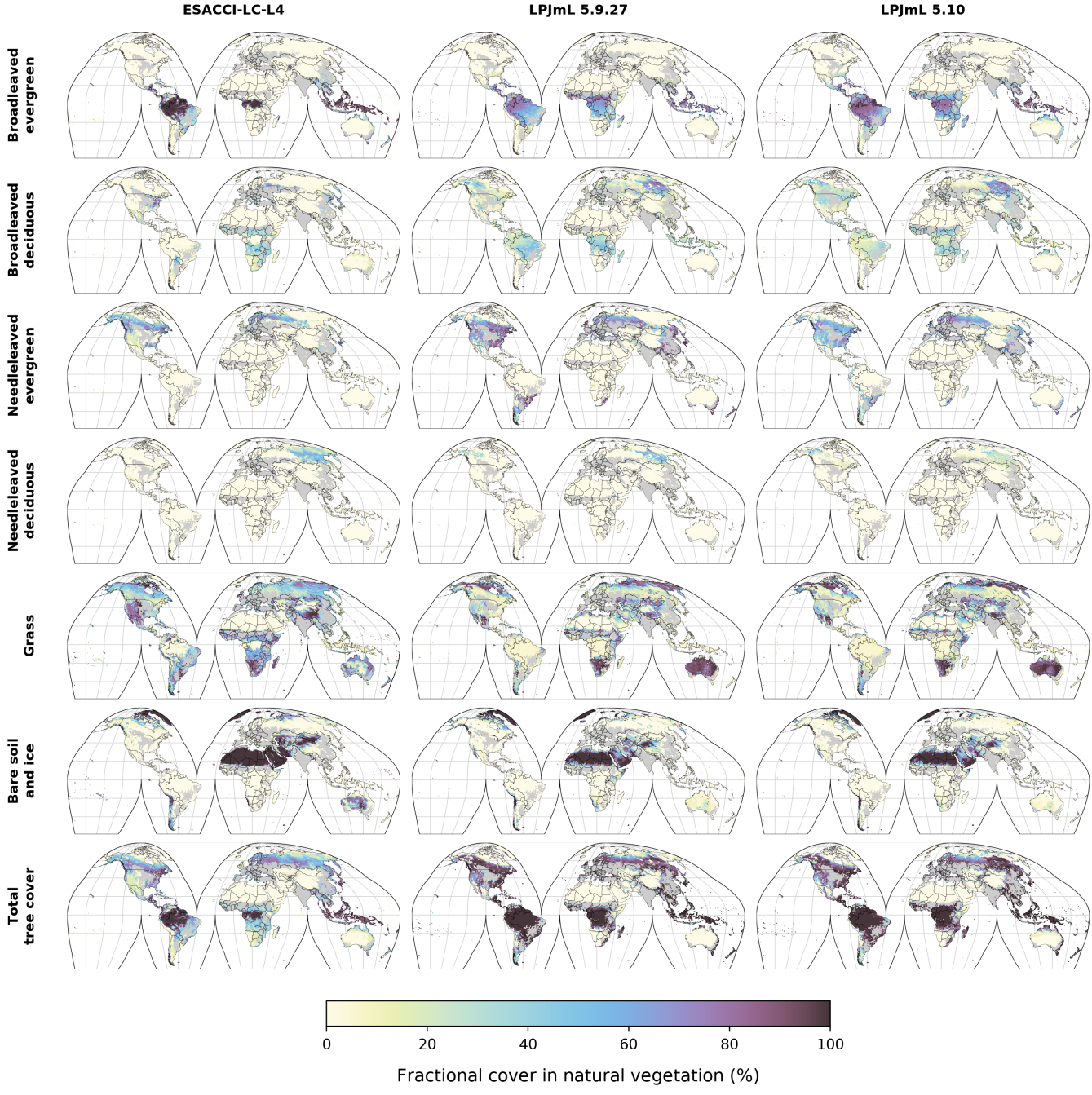

Figure 1. Spatial distribution of vegetation fractions in LPJmL 5.10 compared with ESA CCI LC4 land-cover data (Harper et al., 2023). The figure contrasts simulated and observation-based PFT fractions and highlights regions where the updated model changes tropical evergreen–raingreen partitioning, boreal tree composition, and open vegetation cover.

https://doi.org/10.5194/egusphere-2026-4549
Preprint. Discussion started: 28 September 2026

water-balance response is smaller than the C–N response: transpiration decreases by 5%, while evaporation, interception, and runoff increase by less than 3%.

3.6 Comparison with literature estimates

We compared selected N losses and BNF from LPJmL 5.9.27 and LPJmL 5.10 with published global estimates to assess whether the revised N cycle produces plausible absolute fluxes (Table 6). The comparison suggests an improvement in LPJmL 5.10 for the two largest gaseous and hydrological N loss pathways. Leaching increases from 67 to 88 $\mathrm{TgN\ yr^{-1}}$, moving from below the literature range into agreement with the higher estimate, and N_2 emissions increase from 48 to 64 $\mathrm{TgN\ yr^{-1}}$, closely matching the lower end of the literature range. N_2O emissions remain within the broad literature range in both versions. Volatilization is overestimated relative to literature in both versions, though slightly less so in LPJmL 5.10. BNF is similar in both versions and somewhat above the upper end of the broad literature range.

3.7 Transient nitrogen balance

Following the N-balance analysis of Wirth et al. (2024), we interpret the transient simulations as a balance over vegetation and soil N pools, including organic and mineral forms of N. Inputs comprise atmospheric deposition, BNF, manure, synthetic fertilizer, and establishment fluxes, whereas losses comprise leaching, volatilization, N_2 and N_2O emissions, fire, harvest, and land-use-change emissions. This balance perspective is useful because the net N balance can remain relatively small even when individual input and loss pathways change.

Figure 2 shows that LPJmL 5.10 establishes a different internal partitioning of the N cycle than LPJmL 5.9.27. The lower plant N uptake is not a short-term adjustment after spinup, but persists throughout the transient period, consistent with the reduced vegetation N stocks in Table 5. At the same time, mineral soil N shifts towards a larger NO_3^- pool, which increases the potential for leaching and denitrification losses. The land-use simulation further combines these internal changes with rising anthropogenic N inputs after the mid-20th century, so that fertilizer and manure inputs are partly balanced by larger harvest removals and N losses. These transient balance patterns therefore indicate that the revised demand and uptake formulations do not merely change the 2001–2010 mean fluxes in Table 6; they alter the transient N-cycle state by reducing vegetation N accumulation and increasing the availability of mineral N in soils.

https://doi.org/10.5194/egusphere-2026-4549
Preprint. Discussion started: 28 September 2026

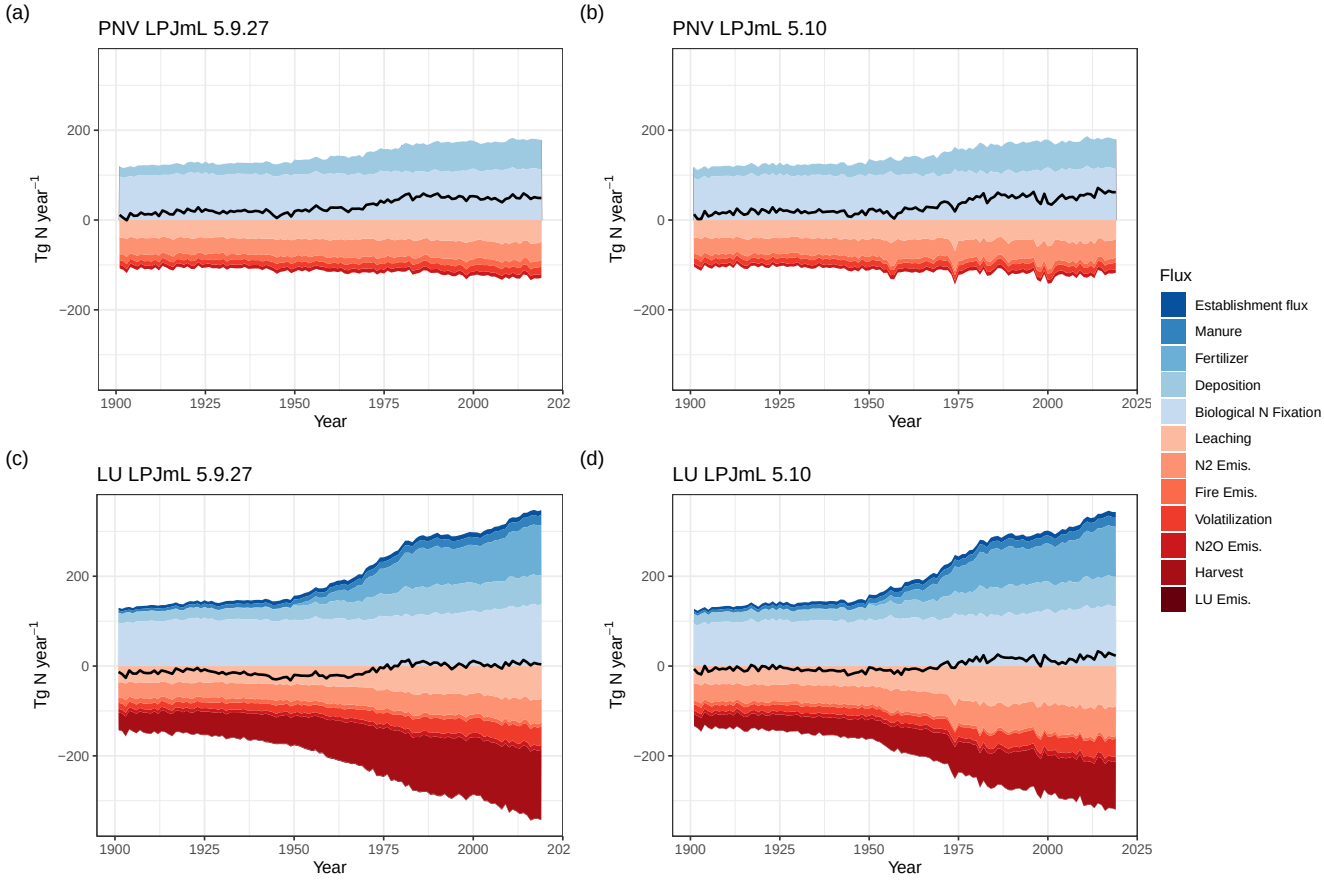

Figure 2. Transient global terrestrial nitrogen-balance components in LPJmL 5.9.27 and LPJmL 5.10, following the balance structure of Wirth et al. (2024). Inputs include deposition, biological nitrogen fixation, manure, synthetic fertilizer, and establishment fluxes; losses include leaching, volatilization, N_2 and N_2O emissions, fire, harvest, and land-use-change emissions. Black line denotes the net balance.

https://doi.org/10.5194/egusphere-2026-4549
Preprint. Discussion started: 28 September 2026

Table 3. ILAMB scores for model versions 5.9.27 and 5.10. Scores range from 0 to 1, with higher values indicating better agreement with the reference data. Blank cells indicate score components not provided for the corresponding benchmark data set.

	Bias		RMSE		Seasonal Cyc.		Spatial Dist.		Overall	
	5.9.27	5.10	5.9.27	5.10	5.9.27	5.10	5.9.27	5.10	5.9.27	5.10
Ecosystem and Carbon Cycle										
Biomass										
ESACCI	0.574	0.579					0.608	0.587	0.591	0.583
GEOCARBON	0.547	0.542					0.528	0.513	0.538	0.527
NBCD2000	0.621	0.581					0.769	0.607	0.695	0.594
Thurner	0.598	0.584					0.884	0.836	0.741	0.710
Tropical	0.667	0.670					0.926	0.927	0.797	0.798
XuSaatchi	0.040	0.041					0.904	0.909	0.472	0.475
Mean	0.508	0.499					0.770	0.730	0.639	0.615
Gross Primary Productivity										
FLUXCOM	0.507	0.492	0.431	0.382	0.791	0.798	0.914	0.931	0.614	0.597
FLUXNET2015	0.613	0.605	0.439	0.431	0.837	0.865			0.582	0.583
WECANN	0.574	0.559	0.439	0.390	0.771	0.774	0.960	0.946	0.637	0.612
Mean	0.565	0.552	0.436	0.401	0.800	0.812	0.937	0.939	0.611	0.597
Net Ecosystem Exchange										
FLUXCOM	0.323	0.332	0.329	0.305	0.751	0.799	0.131	0.148	0.373	0.378
FLUXNET2015	0.490	0.483	0.379	0.376	0.699	0.705			0.487	0.485
Mean	0.406	0.407	0.354	0.341	0.725	0.752	0.131	0.148	0.430	0.431
Soil Carbon										
HWSD	0.481	0.462					0.295	0.215	0.388	0.339
NCSCDV22	0.453	0.408					0.555	0.446	0.504	0.427
Mean	0.467	0.435					0.425	0.331	0.446	0.383
Hydrology Cycle										
Evapotranspiration										
GLEAMv3.3a	0.633	0.599	0.594	0.574	0.854	0.804	0.964	0.955	0.728	0.701
MOD16A2	0.564	0.541	0.512	0.488	0.765	0.746	0.975	0.971	0.666	0.647
MODIS	0.565	0.542	0.513	0.488	0.764	0.743	0.975	0.971	0.666	0.647
Mean	0.587	0.561	0.540	0.517	0.794	0.764	0.971	0.966	0.687	0.665
Runoff										
Dai	0.769	0.747					0.960	0.960	0.769	0.759
LORA	0.471	0.466	0.363	0.365	0.848	0.849	0.923	0.922	0.594	0.593
Mean	0.620	0.607	0.363	0.365	0.848	0.849	0.942	0.941	0.681	0.676
Radiation and Energy Cycle										
Albedo										
CERES	0.376	0.377	0.468	0.469	0.651	0.651	0.933	0.934	0.579	0.580
CERESed4.2	0.348	0.355	0.455	0.462	0.612	0.631	0.915	0.917	0.557	0.566
GEWEX.SRB	0.398	0.402	0.529	0.536	0.586	0.613	0.968	0.968	0.602	0.611
Mean	0.374	0.378	0.484	0.489	0.616	0.632	0.939	0.940	0.579	0.586
Latent Heat Flux										
FLUXCOM	0.586	0.568	0.597	0.585	0.893	0.886	0.984	0.979	0.732	0.721
FLUXNET2015	0.669	0.653	0.475	0.478	0.887	0.895			0.627	0.626
WECANN	0.640	0.633	0.588	0.582	0.847	0.855	0.984	0.984	0.730	0.727
Mean	0.632	0.618	0.553	0.548	0.876	0.879	0.984	0.982	0.696	0.691

https://doi.org/10.5194/egusphere-2026-4549
Preprint. Discussion started: 28 September 2026

Table 4. ILAMB scores for relationships with precipitation and temperature for model versions 5.9.27 and 5.10. Scores range from 0 to 1, with higher values indicating a closer match to the reference relationship. Blank cells indicate relationship diagnostics not provided for the corresponding benchmark data set.

	Precipitation		Temperature		Overall	
	5.9.27	5.10	5.9.27	5.10	5.9.27	5.10
Ecosystem and Carbon Cycle						
Biomass						
ESACCI	0.715	0.698	0.614	0.611	0.665	0.655
GEOCARBON	0.584	0.575	0.495	0.483	0.539	0.529
NBCD2000	0.637	0.618	0.611	0.545	0.624	0.582
Thurner	0.690	0.675	0.594	0.549	0.642	0.612
XuSaatchi	0.745	0.757	0.731	0.742	0.738	0.749
Mean	0.674	0.665	0.609	0.586	0.642	0.625
Gross Primary Productivity						
FLUXCOM	0.838	0.863	0.713	0.692	0.775	0.777
WECANN			0.792	0.742	0.792	0.742
Mean	0.838	0.863	0.752	0.717	0.784	0.760
Hydrology Cycle						
Evapotranspiration						
GLEAMv3.3a	0.848	0.826	0.819	0.804	0.834	0.815
MOD16A2	0.890	0.867	0.769	0.760	0.830	0.813
MODIS	0.892	0.868	0.769	0.760	0.830	0.814
Mean	0.877	0.854	0.786	0.775	0.831	0.814

https://doi.org/10.5194/egusphere-2026-4549
Preprint. Discussion started: 28 September 2026

Table 5. Global benchmark variables for the transient land-use (LU) simulation, comparing LPJmL 5.9.27 and LPJmL 5.10. Values are averages over 1991–2000.

variable	unit	LPJmL 5.9.27	LPJmL 5.10	difference	% difference
Vegetation C	[GtC]	423.7	418.1	-5.636	-1.33
Soil C	[GtC]	2558	2789	230.7	9.019
Litter C	[GtC]	162.6	165.7	3.053	1.877
GPP	[$\mathrm{GtC\,yr^{-1}}$]	128.4	137.5	9.062	7.058
NPP	[$\mathrm{GtC\,yr^{-1}}$]	62.82	67.56	4.744	7.552
NEP	[$\mathrm{GtC\,yr^{-1}}$]	6.633	7.231	0.598	9.018
NBP	[$\mathrm{GtC\,yr^{-1}}$]	0.8198	1.261	0.441	53.79
Harvest C	[$\mathrm{GtC\,yr^{-1}}$]	3.872	3.819	-0.05287	-1.366
Fire C	[$\mathrm{GtC\,yr^{-1}}$]	1.896	2.142	0.2455	12.95
Vegetation N	[GtN]	3.64	2.374	-1.265	-34.77
Soil N	[GtN]	158	165.7	7.718	4.884
Soil NH_4^+	[GtN]	3.674	2.66	-1.014	-27.6
Soil NO_3^-	[GtN]	2.066	4.868	2.803	135.7
N leaching	[$\mathrm{GtN\,yr^{-1}}$]	0.06242	0.08384	0.02142	34.31
N immobilization	[$\mathrm{GtN\,yr^{-1}}$]	1.014	1.203	0.1889	18.63
N mineralization	[$\mathrm{GtN\,yr^{-1}}$]	2.046	1.884	-0.1618	-7.907
N volatilization	[$\mathrm{GtN\,yr^{-1}}$]	0.03252	0.03107	-0.001443	-4.439
N_2 emissions	[$\mathrm{GtN\,yr^{-1}}$]	0.04694	0.06004	0.0131	27.9
N_2O emissions (denitrification)	[$\mathrm{GtN\,yr^{-1}}$]	0.005802	0.007421	0.001619	27.9
N_2O emissions (nitrification)	[$\mathrm{GtN\,yr^{-1}}$]	0.003899	0.003241	-0.0006581	-16.88
N uptake	[$\mathrm{GtN\,yr^{-1}}$]	1.071	0.6856	-0.3858	-36.01
BNF	[$\mathrm{GtN\,yr^{-1}}$]	0.1187	0.1191	0.0004446	0.3746
Evaporation	[$\mathrm{km^3\,yr^{-1}}$]	12646	12968	322.7	2.552
Transpiration	[$\mathrm{km^3\,yr^{-1}}$]	38750	36788	-1962	-5.062
Interception	[$\mathrm{km^3\,yr^{-1}}$]	10540	10771	231	2.192
Runoff	[$\mathrm{km^3\,yr^{-1}}$]	50350	51715	1365	2.711

https://doi.org/10.5194/egusphere-2026-4549
Preprint. Discussion started: 28 September 2026

Table 6. Comparison of 2001 to 2010 average global N fluxes from LPJmL 5.9.27 and LPJmL 5.10 (land-use simulation) against published literature estimates. Literature estimates are available only for selected fluxes.

	LPJmL 5.9.27 LU	*LPJmL 5.10 LU*	Literature
N losses ($\mathrm{TgN\ yr^{-1}}$)			
Leaching	67.1	88.1	93[1], 68[2]
Volatilization	36.1	34.2	21.4[3,4]
N_2 emissions	48.4	64.2	68[1], 64.2[2]
N_2O emissions	9.9	11.2	10.9[5], 13[6], 10[7], 7.4-12.3[8], 12.9[9]
BNF	126	125	19.8-107.9[10]

[1]Bouwman et al. (2013), [2]Zaehle et al. (2010), [3]volatilization from natural soils (2.4 $\mathrm{TgN\ yr^{-1}}$) from Bouwman et al. (2002), [4]volatilization from manure and synthetic fertiliser on crop- and grasslands (19 $\mathrm{TgN\ yr^{-1}}$) from Bouwman et al. (1997), [5]Galloway et al. (2004), [6]Sutton et al. (2013), [7]Tian et al. (2019), [8]Tian et al. (2020), [9]Scheer et al. (2020), [10]Yu and Zhuang (2020b)

https://doi.org/10.5194/egusphere-2026-4549
Preprint. Discussion started: 28 September 2026

4 Discussion

The update from version 5.9.27 to version 5.10 corrects the computation of N demand, which is a fundamentally important component of the terrestrial N balance and N limitation of plant growth and consequently, the terrestrial carbon cycle. The reduced N demand introduced by this correction is counterbalanced by the improved representation of N uptake and recovery. Although the updated uptake formulation is grounded in literature and empirical data (Craig et al., 2025), the underlying parameters remain loosely constrained. They are largely derived from controlled, artificial experimental setups that do not necessarily reflect N uptake dynamics under natural conditions. While the bug fix and its associated counterbalancing changes do not fundamentally alter overall model performance with respect to the global carbon cycle, N stocks and subsequent loss pathways are modified in version 5.10. Lower N stocks in vegetation pools lead to reduced N recycling. Concurrently, larger mineral soil N pools lead to increased N losses via leaching and gaseous emissions, bringing LPJmL-based estimates into closer agreement with absolute literature values (Table 6). Biological nitrogen fixation (BNF) also responds strongly to the reduced plant N demand. This allows the BNF parameterization in version 5.10 to be less restrictive than in earlier versions (Wirth et al., 2024) while maintaining global BNF estimates within the range reported by Davies-Barnard and Friedlingstein (2020), which we consider a notable conceptual improvement. In contrast to vegetation pools and mineral soil N, soil organic N (SON) is strongly determined by soil organic C pools and target soil C–N ratios. Consequently, reduced organic N input through litterfall is compensated through higher immobilization rates leaving total SON pools largely unchanged. We note an increase in global soil C stocks, driven by an SOC increase in permafrost regions in 5.10 compared to 5.9.27; this heightens disagreement with observational data in ILAMB (Table 3). However, permafrost region soil C stocks tend to be systematically underestimated in those reference data (Tarnocai et al., 2009; Schaphoff et al., 2013), suggesting the model's response may be more realistic than the benchmarks imply.

Beyond improving individual N flux estimates, version 5.10 improves the conceptual basis for N demand in photosynthesis and growth, as well as plant nitrogen acquisition. This establishes a more realistic basis for future model development (e.g., Schaphoff et al., 2026) and applications, as N limitation is an important driver of future vegetation dynamics and the terrestrial C cycle(e.g., Kou-Giesbrecht, 2025; Meyerholt et al., 2020). Similarly, the simulated vegetation distribution improves against reference data (Harper et al., 2023) (Sect. 3.2), reflecting the phenology timing and other parameter revisions described in Sect. 2.3.

While the implemented changes and parameterisation for version 5.10 improve the realism of the represented processes in LPJmL and associated N stocks, there is room for further improvement and better process understanding. N uptake rates as reported by Craig et al. (2025) show great variability and are based on artificial growth conditions that may fail to represent other environmental controls on N uptake. We thus target these parameters as primary candidates for future calibration and model improvement efforts. Similarly, the relationship of carboxylation capacity and leaf N content as reported by Dong et al. (2022) only predicts the N content per leaf area but not the dependence of the carboxylation capacity on available N in the leaves. For simulating N controls on photosynthesis and growth, a relationship in both directions is needed.

LPJmL development has since moved on to version 6.0.0 (Schaphoff et al., 2026), which builds directly on this release.

https://doi.org/10.5194/egusphere-2026-4549
Preprint. Discussion started: 28 September 2026

5 Conclusions

We identified and corrected a structural error in the nitrogen demand formulation of LPJmL that had inflated leaf nitrogen demand by a factor of approximately two, caused by an inappropriate daylength scaling of V_{cmax} inherited from Smith et al. (2014). Correcting this error alone effectively eliminated nitrogen limitation on simulated vegetation growth. Restoring a plausible level of nitrogen limitation therefore required a coordinated package of further revisions to nitrogen uptake kinetics, nitrogen recovery and turnover, and tree phenology; we present this package as LPJmL version 5.10.

Relative to its predecessor, LPJmL 5.9.27, global vegetation nitrogen stocks and nitrogen uptake decrease by around 35% in LPJmL 5.10. Gross and net primary production nonetheless increase by 7–8%: the corrected, lower nitrogen demand more than offsets the reduction in simulated uptake. Mineral soil nitrogen shifts towards a larger nitrate pool, and immobilisation, leaching, and denitrification losses increase accordingly; simulated nitrogen losses move into closer agreement with published estimates as a result. Aggregate land-surface performance for energy and hydrological diagnostics is preserved, and the simulated vegetation distribution improves against satellite-derived land cover.

These results show that other components of the model had effectively been tuned around the presence of the scaling error, so that correcting it in isolation was insufficient. Restoring a coherent nitrogen and carbon balance, together with a plausible vegetation distribution, instead required a coordinated revision of nitrogen supply and demand, carbon allocation, and tree phenology, not a single parameter correction. As the final release of the LPJmL 5 series, version 5.10 documents the exact model configuration used for the TRENDY simulations contributing to the Global Carbon Budget 2025 (Friedlingstein et al., 2026). It also establishes a structurally consistent nitrogen cycle as the basis for the forthcoming LPJmL 6 series (Schaphoff et al., 2026).

Code and data availability. The LPJmL 5.10 code is hosted at github.com under https://github.com/PIK-LPJmL/LPJmL/, and an exact copy of code version 5.10 as described here is archived in the associated Zenodo archive: https://zenodo.org/records/17911585 (Schaphoff et al., 2025). The LPJmL benchmark PDF reports, the full ILAMB report, the ILAMB configuration and output underlying the results in Sect. 3, and the raw LPJmL 5.9.27 and 5.10 model output, together with the model code, are jointly archived on Zenodo: https://doi.org/10.5281/zenodo.21624306 (Heinke et al., 2026). Third-party observational and benchmark data sets used for model evaluation are not redistributed here and must be obtained from the original providers cited in the main text.

https://doi.org/10.5194/egusphere-2026-4549
Preprint. Discussion started: 28 September 2026

Appendix A: Potential natural vegetation benchmark

Table A1. Global benchmark variables for the potential natural vegetation (PNV) simulation, comparing LPJmL 5.9.27 and LPJmL 5.10. Values are averages over 1991–2000.

variable	unit	LPJmL 5.9.27	LPJmL 5.10	difference	% difference
Vegetation C	[GtC]	619.9	594.1	-25.8	-4.162
Soil C	[GtC]	2643	2870	226.7	8.577
Litter C	[GtC]	232.6	224.7	-7.88	-3.388
GPP	$[\mathrm{GtC\,yr^{-1}}]$	142.5	153	10.57	7.422
NPP	$[\mathrm{GtC\,yr^{-1}}]$	66.86	71.32	4.457	6.666
NEP	$[\mathrm{GtC\,yr^{-1}}]$	5.649	6.433	0.783	13.87
NBP	$[\mathrm{GtC\,yr^{-1}}]$	2.602	3.108	0.506	19.45
Fire C	$[\mathrm{GtC\,yr^{-1}}]$	3.047	3.324	0.2773	9.099
Vegetation N	[GtN]	4.611	2.894	-1.718	-37.25
Soil N	[GtN]	163.9	170.3	6.402	3.907
Soil NH_4^+	[GtN]	3.695	2.664	-1.031	-27.9
Soil NO_3^-	[GtN]	2.089	4.434	2.346	112.3
N leaching	$[\mathrm{GtN\,yr^{-1}}]$	0.04722	0.04797	0.0007495	1.587
N immobilization	$[\mathrm{GtN\,yr^{-1}}]$	1.066	1.27	0.2044	19.17
N mineralization	$[\mathrm{GtN\,yr^{-1}}]$	2.31	2.05	-0.2598	-11.25
N volatilization	$[\mathrm{GtN\,yr^{-1}}]$	0.01336	0.01326	-0.0001041	-0.779
N_2 emissions	$[\mathrm{GtN\,yr^{-1}}]$	0.04051	0.04432	0.00381	9.406
N_2O emissions (denitrification)	$[\mathrm{GtN\,yr^{-1}}]$	0.005007	0.005478	0.0004709	9.406
N_2O emissions (nitrification)	$[\mathrm{GtN\,yr^{-1}}]$	0.003698	0.002804	-0.0008942	-24.18
N uptake	$[\mathrm{GtN\,yr^{-1}}]$	1.216	0.7573	-0.4584	-37.71
BNF	$[\mathrm{GtN\,yr^{-1}}]$	0.1097	0.1099	0.0001722	0.157
Evaporation	$[\mathrm{km^3\,yr^{-1}}]$	8394	8905	510.7	6.084
Transpiration	$[\mathrm{km^3\,yr^{-1}}]$	40467	37608	-2860	-7.067
Interception	$[\mathrm{km^3\,yr^{-1}}]$	11668	11471	-196.4	-1.683
Runoff	$[\mathrm{km^3\,yr^{-1}}]$	49745	52299	2553	5.133

https://doi.org/10.5194/egusphere-2026-4549
Preprint. Discussion started: 28 September 2026

Appendix B: Crop modeling performance

Global interannual yield anomaly time series for LPJmL 5.9.27 and LPJmL 5.10, compared against FAOstat and the GGCMI Phase 1 model ensemble (Müller et al., 2017, 2019), are shown below for maize, wheat, rice, and soybean.

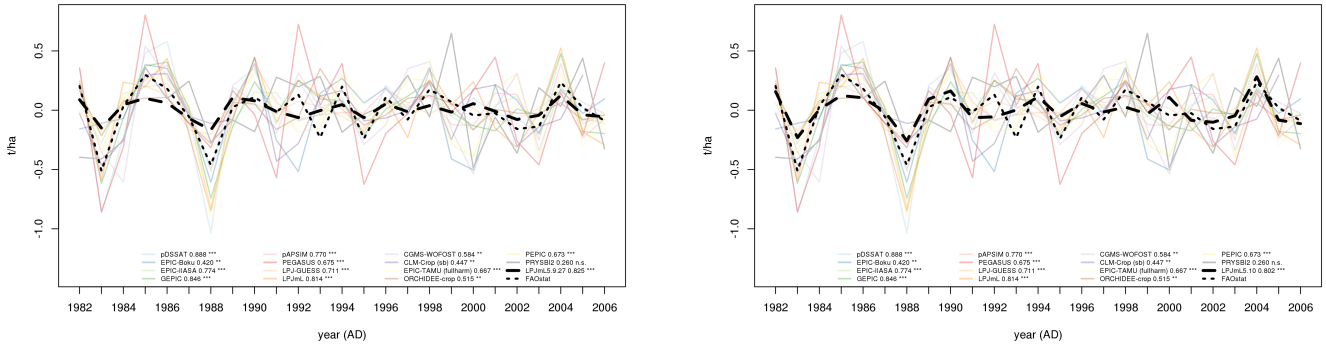

Figure B1. The LPJmL 5.9.27 (left) and 5.10 (right) crop model performance compared against the GGCMI Phase 1 crop model ensemble (Müller et al., 2017, 2019) for maize.

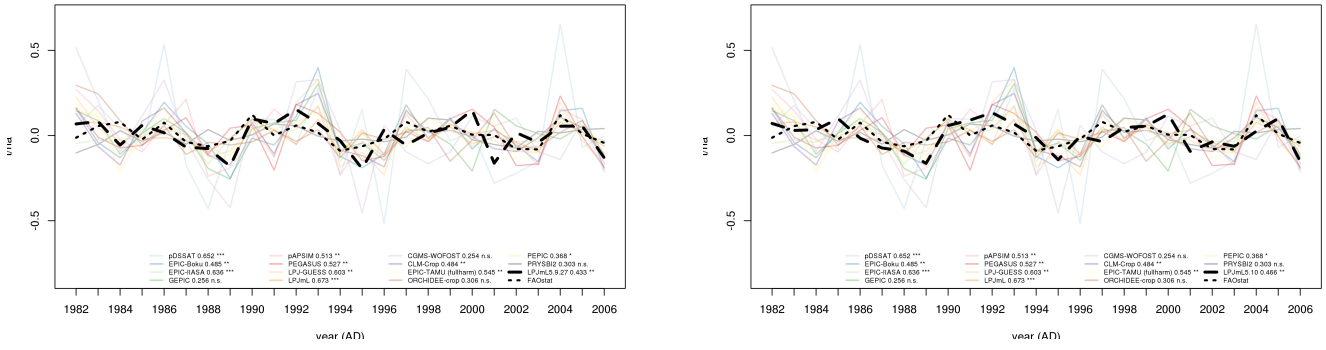

Figure B2. The LPJmL 5.9.27 (left) and 5.10 (right) crop model performance compared against the GGCMI Phase 1 crop model ensemble (Müller et al., 2017, 2019) for wheat.

https://doi.org/10.5194/egusphere-2026-4549
Preprint. Discussion started: 28 September 2026

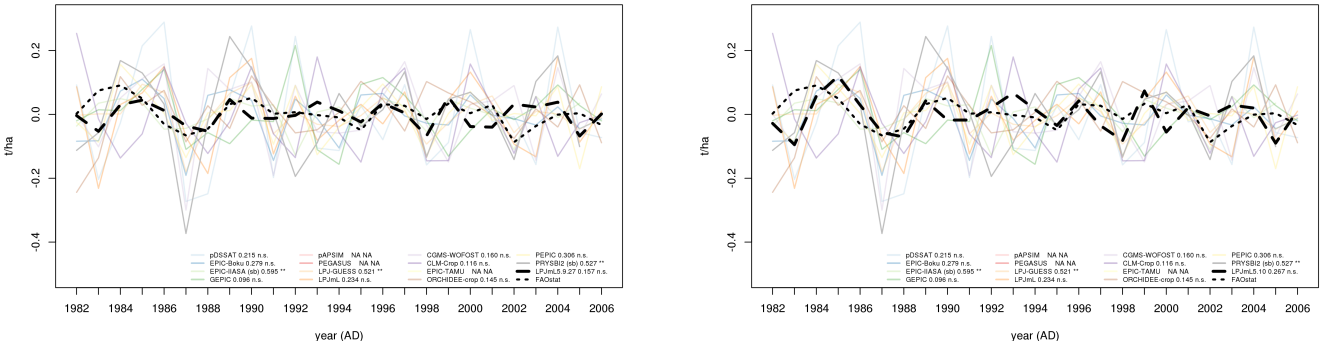

Figure B3. The LPJmL 5.9.27 (left) and 5.10 (right) crop model performance compared against the GGCMI Phase 1 crop model ensemble (Müller et al., 2017, 2019) for rice.

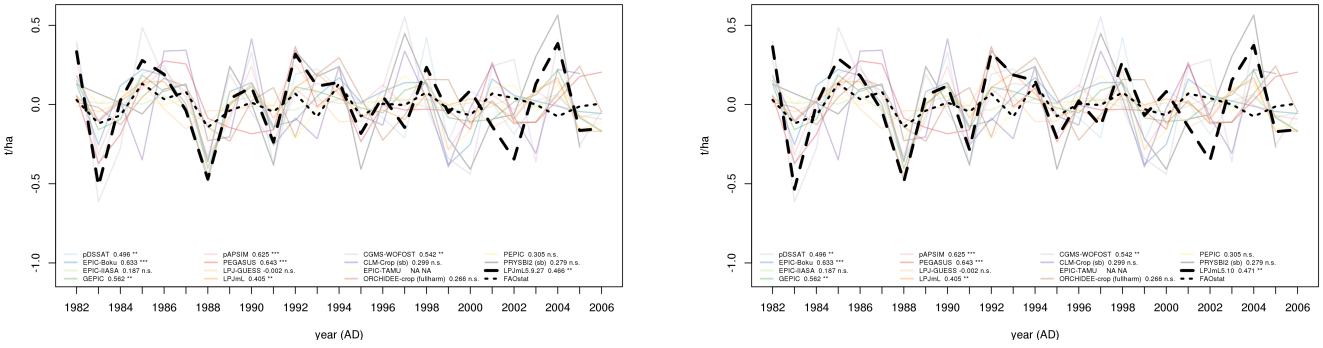

Figure B4. The LPJmL 5.9.27 (left) and 5.10 (right) crop model performance compared against the GGCMI Phase 1 crop model ensemble (Müller et al., 2017, 2019) for soybean.

https://doi.org/10.5194/egusphere-2026-4549
Preprint. Discussion started: 28 September 2026

Author contributions. JH: Conceptualization, Methodology, Writing – Original Draft. All authors: Software, Validation, Writing – Review & Editing.

Competing interests. At least one of the (co-)authors is a member of the editorial board of Geoscientific Model Development.

Acknowledgements. We would like to acknowledge the Ministry of Research, Science and Culture of the State of Brandenburg for providing resources on the high-performance computer system at the Potsdam Institute for Climate Impact Research (Potsdam, Germany). During the preparation of this work, the authors used the large language model Claude (Anthropic) to assist with drafting and revising text, checking internal consistency, and verifying reported values against source data. After using this tool, the authors reviewed and edited the content as needed and take full responsibility for the content of the publication.

Financial support. JH has received funding from the European commission through projects ClimTip (grant no. 101137601) and ESM2025 (grant no. 101003536), and from the Future of Life Institute through the CODEC project. SBW received funding from the German Federal Ministry for Research, technology and Space (BMFTR, projects ABCDR, grant 01LS2105A and CDRfarm, grant 01LS2514A).

https://doi.org/10.5194/egusphere-2026-4549
Preprint. Discussion started: 28 September 2026

References

Bernacchi, C. J., Singsaas, E. L., Pimentel, C., Portis Jr, A. R., and Long, S. P.: Improved Temperature Response Functions for Models of Rubisco-limited Photosynthesis, 24, 253–259, https://doi.org/10.1111/j.1365-3040.2001.00668.x, 2001.

Biemans, H., Haddeland, I., Kabat, P., Ludwig, F., Hutjes, R. W. a., Heinke, J., von Bloh, W., and Gerten, D.: Impact of reservoirs on river discharge and irrigation water supply during the 20th century, Water Resources Research, 47, W03 509, https://doi.org/10.1029/2009WR008929, 2011.

Bondeau, A., Smith, P. C., Zaehle, S., Schaphoff, S., Lucht, W., Cramer, W., Gerten, D., Lotze-Campen, H., Müller, C., Reichstein, M., and Smith, B.: Modelling the role of agriculture for the 20th century global terrestrial carbon balance, Global Change Biol., 13, 679–706, https://doi.org/10.1111/j.1365-2486.2006.01305.x, 2007.

Bouwman, A. F., Lee, D. S., Asman, W. a. H., Dentener, F. J., Van Der Hoek, K. W., and Olivier, J. G. J.: A Global High-Resolution Emission Inventory for Ammonia, Glob. Biogeochem. Cycles, 11, 561–587, https://doi.org/10.1029/97GB02266, 1997.

Bouwman, A. F., Boumans, L. J. M., and Batjes, N. H.: Estimation of Global NH3 Volatilization Loss from Synthetic Fertilizers and Animal Manure Applied to Arable Lands and Grasslands, Glob. Biogeochem. Cycles, 16, 8–1–8–14, https://doi.org/10.1029/2000GB001389, 2002.

Bouwman, A. F., Beusen, A. H. W., Griffioen, J., Van Groenigen, J. W., Hefting, M. M., Oenema, O., Van Puijenbroek, P. J. T. M., Seitzinger, S., Slomp, C. P., and Stehfest, E.: Global Trends and Uncertainties in Terrestrial Denitrification and N2O Emissions, Philos. Trans. R. Soc. B Biol. Sci., 368, 20130 112, https://doi.org/10.1098/rstb.2013.0112, 2013.

Craig, M. E., Walker, A. P., Iversen, C. M., Knox, R. G., Yaffar, D., and York, L. M.: Tree Root Nutrient Uptake Kinetics Vary with Nutrient Availability, Environmental Conditions, and Root Traits: A Global Analysis, New Phytologist, 246, 2495–2505, https://doi.org/10.1111/nph.70140, 2025.

Cucchi, M., Weedon, G. P., Amici, A., Bellouin, N., Lange, S., Müller Schmied, H., Hersbach, H., and Buontempo, C.: WFDE5: bias-adjusted ERA5 reanalysis data for impact studies, Earth System Science Data, 12, 2097–2120, https://doi.org/10.5194/essd-12-2097-2020, 2020.

Davies-Barnard, T. and Friedlingstein, P.: The Global Distribution of Biological Nitrogen Fixation in Terrestrial Natural Ecosystems, Global Biogeochem. Cycles, 34, e2019GB006 387, https://doi.org/10.1029/2019GB006387, 2020.

De Pury, D. G. G. and Farquhar, G. D.: Simple Scaling of Photosynthesis from Leaves to Canopies without the Errors of Big-leaf Models, 20, 537–557, https://doi.org/10.1111/j.1365-3040.1997.00094.x, 1997.

Dong, N., Prentice, I. C., Wright, I. J., Wang, H., Atkin, O. K., Bloomfield, K. J., Domingues, T. F., Gleason, S. M., Maire, V., Onoda, Y., Poorter, H., and Smith, N. G.: Leaf Nitrogen from the Perspective of Optimal Plant Function, 110, 2585–2602, https://doi.org/10.1111/1365-2745.13967, 2022.

FAO: AQUASTAT database, Food and Agriculture Organization of the United Nations, Rome, http://www.fao.org/nr/water/aquastat/data/query/index.html?lang=en, accessed 2020-04-17, 2020a.

FAO: FAOSTAT database, Food and Agriculture Organization of the United Nations, Rome, http://www.fao.org/faostat/en/, accessed 2020-01-27, 2020b.

FAO/IIASA/ISRIC/ISSCAS/JRC: Harmonized World Soil Database (version 1.21), FAO, Rome, Italy and IIASA, Laxenburg, Austria, https://iiasa.ac.at/web/home/research/researchPrograms/water/HWSD.html, accessed 2021-03-11, 2012.

Field, C. and Mooney, H. A.: The Photosynthesis-Nitrogen Relationship in Wild Plants, in: On the Economy of Plant Form and Function, edited by Givnish, T. J., pp. 25–55, Cambridge University Press, 1986.

https://doi.org/10.5194/egusphere-2026-4549
Preprint. Discussion started: 28 September 2026

Flörke, M., Kynast, E., Bärlund, I., Eisner, S., Wimmer, F., and Alcamo, J.: Domestic and industrial water uses of the past 60 years as a mirror of socio-economic development: A global simulation study, Global Environmental Change, 23, 144–156, https://doi.org/10.1016/j.gloenvcha.2012.10.018, 2013.

Forkel, M., Carvalhais, N., Schaphoff, S., V. Bloh, W., Migliavacca, M., Thurner, M., and Thonicke, K.: Identifying environmental controls on vegetation greenness phenology through model–data integration, Biogeosciences, 11, 7025–7050, https://doi.org/10.5194/bg-11-7025-2014, 2014.

Friedlingstein, P., O'Sullivan, M., Jones, M. W., Andrew, R. M., Bakker, D. C. E., Hauck, J., Landschützer, P., Le Quéré, C., Luijkx, I. T., Peters, G. P., Peters, W., Pongratz, J., Schwingshackl, C., Sitch, S., Canadell, J. G., Ciais, P., Jackson, R. B., Alin, S. R., Anthoni, P., Barbero, L., Bates, N. R., Becker, M., Bellouin, N., Decharme, B., Bopp, L., Brasika, I. B. M., Cadule, P., Chamberlain, M. A., Chandra, N., Chau, T.-T.-T., Chevallier, F., Chini, L. P., Cronin, M., Dou, X., Enyo, K., Evans, W., Falk, S., Feely, R. A., Feng, L., Ford, D. J., Gasser, T., Ghattas, J., Gkritzalis, T., Grassi, G., Gregor, L., Gruber, N., Gürses, O., Harris, I., Hefner, M., Heinke, J., Houghton, R. A., Hurtt, G. C., Iida, Y., Ilyina, T., Jacobson, A. R., Jain, A., Jarníková, T., Jersild, A., Jiang, F., Jin, Z., Joos, F., Kato, E., Keeling, R. F., Kennedy, D., Klein Goldewijk, K., Knauer, J., Korsbakken, J. I., Körtzinger, A., Lan, X., Lefèvre, N., Li, H., Liu, J., Liu, Z., Ma, L., Marland, G., Mayot, N., McGuire, P. C., McKinley, G. A., Meyer, G., Morgan, E. J., Munro, D. R., Nakaoka, S.-I., Niwa, Y., O'Brien, K. M., Olsen, A., Omar, A. M., Ono, T., Paulsen, M., Pierrot, D., Pocock, K., Poulter, B., Powis, C. M., Rehder, G., Resplandy, L., Robertson, E., Rödenbeck, C., Rosan, T. M., Schwinger, J., Séférian, R., Smallman, T. L., Smith, S. M., Sospedra-Alfonso, R., Sun, Q., Sutton, A. J., Sweeney, C., Takao, S., Tans, P. P., Tian, H., Tilbrook, B., Tsujino, H., Tubiello, F., van der Werf, G. R., van Ooijen, E., Wanninkhof, R., Watanabe, M., Wimart-Rousseau, C., Yang, D., Yang, X., Yuan, W., Yue, X., Zaehle, S., Zeng, J., and Zheng, B.: Global Carbon Budget 2023, Earth System Science Data, 15, 5301–5369, https://doi.org/10.5194/essd-15-5301-2023, 2023.

Friedlingstein, P., O'Sullivan, M., Jones, M. W., Andrew, R. M., Bakker, D. C. E., Hauck, J., Landschützer, P., Le Quéré, C., Li, H., Luijkx, I. T., Peters, G. P., Peters, W., Pongratz, J., Schwingshackl, C., Sitch, S., Canadell, J. G., Ciais, P., Aas, K., Alin, S. R., Anthoni, P., Barbero, L., Bates, N. R., Bellouin, N., Benoit-Cattin, A., Berghoff, C. F., Bernardello, R., Bopp, L., Brasika, I. B. M., Chamberlain, M. A., Chandra, N., Chevallier, F., Chini, L. P., Collier, N. O., Colligan, T. H., Cronin, M., Djeutchouang, L., Dou, X., Enright, M. P., Enyo, K., Erb, M., Evans, W., Feely, R. A., Feng, L., Ford, D. J., Foster, A., Fransner, F., Gasser, T., Gehlen, M., Gkritzalis, T., Goncalves De Souza, J., Grassi, G., Gregor, L., Gruber, N., Guenet, B., Gürses, Ö., Harrington, K., Harris, I., Heinke, J., Hurtt, G. C., Iida, Y., Ilyina, T., Ito, A., Jacobson, A. R., Jain, A. K., Jarníková, T., Jersild, A., Jiang, F., Jones, S. D., Kato, E., Keeling, R. F., Klein Goldewijk, K., Knauer, J., Kong, Y., Korsbakken, J. I., Koven, C., Kunimitsu, T., Lan, X., Liu, J., Liu, Z., Liu, Z., Lo Monaco, C., Ma, L., Marland, G., McGuire, P. C., McKinley, G. A., Melton, J., Monacci, N., Monier, E., Morgan, E. J., Munro, D. R., Müller, J. D., Nakaoka, S.-I., Nayagam, L. R., Niwa, Y., Nutzel, T., Olsen, A., Omar, A. M., Pan, N., Pandey, S., Pierrot, D., Qin, Z., Regnier, P. A. G., Rehder, G., Resplandy, L., Roobaert, A., Rosan, T. M., Rödenbeck, C., Schwinger, J., Skjelvan, I., Smallman, T. L., Spada, V., Sreeush, M. G., Sun, Q., Sutton, A. J., Sweeney, C., Swingedouw, D., Séférian, R., Takao, S., Tatebe, H., Tian, H., Tian, X., Tilbrook, B., Tsujino, H., Tubiello, F., van Ooijen, E., van der Werf, G., van de Velde, S. J., Walker, A., Wanninkhof, R., Yang, X., Yuan, W., Yue, X., and Zeng, J.: Global Carbon Budget 2025, Earth Syst. Sci. Data, 18, 3211–3288, https://doi.org/10.5194/essd-18-3211-2026, 2026.

Galloway, J. N., Dentener, F. J., Capone, D. G., Boyer, E. W., Howarth, R. W., Seitzinger, S. P., Asner, G. P., Cleveland, C. C., Green, P. A., Holland, E. A., Karl, D. M., Michaels, A. F., Porter, J. H., Townsend, A. R., and Vöosmarty, C. J.: Nitrogen Cycles: Past, Present, and Future, Biogeochemistry, 70, 153–226, https://doi.org/10.1007/s10533-004-0370-0, 2004.

Gerten, D., Schaphoff, S., Haberlandt, U., Lucht, W., and Sitch, S.: Terrestrial vegetation and water balance—hydrological evaluation of a dynamic global vegetation model, J. Hydrol., 286, 249–270, https://doi.org/10.1016/j.jhydrol.2003.09.029, 2004.

https://doi.org/10.5194/egusphere-2026-4549
Preprint. Discussion started: 28 September 2026

Harper, K. L., Lamarche, C., Hartley, A., Peylin, P., Ottlé, C., Bastrikov, V., San Martín, R., Bohnenstengel, S. I., Kirches, G., Boettcher, M., Shevchuk, R., Brockmann, C., and Defourny, P.: A 29-year time series of annual 300 m resolution plant-functional-type maps for climate models, Earth System Science Data, 15, 1465–1499, https://doi.org/10.5194/essd-15-1465-2023, 2023.

Haxeltine, A. and Prentice, I. C.: A General Model for the Light-Use Efficiency of Primary Production, Functional Ecology, 10, 551, https://doi.org/10.2307/2390165, 1996.

Heinke, J.: A livestock density input for LPJmL5.5, https://doi.org/10.5281/zenodo.14946695, 2025.

Heinke, J., Rolinski, S., and Müller, C.: Modelling the role of livestock grazing in C and N cycling in grasslands with LPJmL5.0-grazing, Geosci. Model Dev., 16, 2455–2475, https://doi.org/10.5194/gmd-16-2455-2023, 2023.

Heinke, J., Schaphoff, S., Wirth, S. B., and Müller, C.: Code and data for: "Revised nitrogen balance for plant photosynthesis and growth in the dynamic global vegetation, hydrology and agriculture model LPJmL (5.10)", https://doi.org/10.5281/zenodo.21624306, 2026.

Herzfeld, T., Heinke, J., Rolinski, S., and Müller, C.: Soil organic carbon dynamics from agricultural management practices under climate change, Earth Syst. Dyn., 12, 1037–1055, https://doi.org/10.5194/esd-12-1037-2021, 2021.

Hurtt, G. C., Chini, L., Sahajpal, R., Frolking, S., Bodirsky, B. L., Calvin, K., Doelman, J. C., Fisk, J., Fujimori, S., Klein Goldewijk, K., Hasegawa, T., Havlik, P., Heinimann, A., Humpenöder, F., Jungclaus, J., Kaplan, J. O., Kennedy, J., Krisztin, T., Lawrence, D., Lawrence, P., Ma, L., Mertz, O., Pongratz, J., Popp, A., Poulter, B., Riahi, K., Shevliakova, E., Stehfest, E., Thornton, P., Tubiello, F. N., van Vuuren, D. P., and Zhang, X.: Harmonization of global land use change and management for the period 850–2100 (LUH2) for CMIP6, Geosci. Model Dev., 13, 5425–5464, https://doi.org/10.5194/gmd-13-5425-2020, data available at https://luh.umd.edu/, accessed 2021-07-08, 2020.

IIASA/FAO: Global Agro-ecological Zones (GAEZv3.0), IIASA, Laxenburg, Austria and FAO, Rome, Italy, http://www.gaez.iiasa.ac.at/, accessed 2020-07-17, 2012.

Jägermeyr, J., Gerten, D., Heinke, J., Schaphoff, S., Kummu, M., and Lucht, W.: Water savings potentials of irrigation systems: global simulation of processes and linkages, Hydrol. Earth Syst. Sci., 19, 3073–3091, https://doi.org/10.5194/hess-19-3073-2015, 2015.

Jägermeyr, J., Gerten, D., Schaphoff, S., Heinke, J., Lucht, W., and Rockström, J.: Integrated crop water management might sustainably halve the global food gap, Environ. Res. Lett., 11, 025 002, https://doi.org/10.1088/1748-9326/11/2/025002, 2016.

Jägermeyr, J., Müller, C., Minoli, S., Ray, D., and Siebert, S.: GGCMI Phase 3 crop calendar, https://doi.org/10.5281/zenodo.5062513, 2021.

Kattge, J., Díaz, S., Lavorel, S., Prentice, I. C., Leadley, P., Bönisch, G., Garnier, E., Westoby, M., Reich, P. B., Wright, I. J., Cornelissen, J. H., Violle, C., Harrison, S. P., Van Bodegom, P. M., Reichstein, M., Enquist, B. J., Soudzilovskaia, N. A., Ackerly, D. D., Anand, M., Atkin, O., Bahn, M., Baker, T. R., Baldocchi, D., Bekker, R., Blanco, C. C., Blonder, B., Bond, W. J., Bradstock, R., Bunker, D. E., Casanoves, F., Cavender-Bares, J., Chambers, J. Q., Chapin, F. S., Chave, J., Coomes, D., Cornwell, W. K., Craine, J. M., Dobrin, B. H., Duarte, L., Durka, W., Elser, J., Esser, G., Estiarte, M., Fagan, W. F., Fang, J., Fernández-Méndez, F., Fidelis, A., Finegan, B., Flores, O., Ford, H., Frank, D., Freschet, G. T., Fyllas, N. M., Gallagher, R. V., Green, W. A., Gutierrez, A. G., Hickler, T., Higgins, S. I., Hodgson, J. G., Jalili, A., Jansen, S., Joly, C. A., Kerkhoff, A. J., Kirkup, D., Kitajima, K., Kleyer, M., Klotz, S., Knops, J. M., Kramer, K., Kühn, I., Kurokawa, H., Laughlin, D., Lee, T. D., Leishman, M., Lens, F., Lenz, T., Lewis, S. L., Lloyd, J., Llusià, J., Louault, F., Ma, S., Mahecha, M. D., Manning, P., Massad, T., Medlyn, B. E., Messier, J., Moles, A. T., Müller, S. C., Nadrowski, K., Naeem, S., Niinemets, Ü., Nöllert, S., Nüske, A., Ogaya, R., Oleksyn, J., Onipchenko, V. G., Onoda, Y., Ordoñez, J., Overbeck, G., Ozinga, W. A., Patiño, S., Paula, S., Pausas, J. G., Peñuelas, J., Phillips, O. L., Pillar, V., Poorter, H., Poorter, L., Poschlod, P., Prinzing, A., Proulx, R., Rammig, A., Reinsch, S., Reu, B., Sack, L., Salgado-Negret, B., Sardans, J., Shiodera, S., Shipley, B., Siefert, A., Sosinski, E., Soussana, J. F., Swaine, E., Swenson, N., Thompson, K., Thornton, P., Waldram, M., Weiher, E., White, M., White, S., Wright, S. J., Yguel, B., Zaehle, S., Zanne, A. E., and Wirth,

https://doi.org/10.5194/egusphere-2026-4549
Preprint. Discussion started: 28 September 2026

C.: TRY - a Global Database of Plant Traits, Global Change Biology, 17, 2905–2935, https://doi.org/10.1111/j.1365-2486.2011.02451.x, 2011.

Kim, H.: Global Soil Wetness Project Phase 3 Atmospheric Boundary Conditions (Experiment 1) [Data set], https://doi.org/10.20783/DIAS.501, 2017.

Klein Goldewijk, K., Beusen, A., Doelman, J., and Stehfest, E.: Anthropogenic land use estimates for the Holocene - HYDE 3.2, Earth Syst. Sci. Data, 9, 927–953, https://doi.org/10.5194/essd-9-927-2017, data available at https://www.pbl.nl/en/image/links/hyde, accessed 2017-10-25, 2017.

Kou-Giesbrecht, S.: Nitrogen Cycling in Earth System Models: From Constraining Carbon Budgets to Projecting Pollution for Planetary Stewardship, J. Geophys. Res. Biogeosci., 130, e2025JG009 209, https://doi.org/10.1029/2025JG009209, 2025.

Kou-Giesbrecht, S., Arora, V. K., Seiler, C., Arneth, A., Falk, S., Jain, A. K., Joos, F., Kennedy, D., Knauer, J., Sitch, S., O'Sullivan, M., Pan, N., Sun, Q., Tian, H., Vuichard, N., and Zaehle, S.: Evaluating nitrogen cycling in terrestrial biosphere models: a disconnect between the carbon and nitrogen cycles, Earth Syst. Dyn., 14, 767–795, https://doi.org/10.5194/esd-14-767-2023, 2023.

Lange, S., Menz, C., Gleixner, S., Cucchi, M., Weedon, G. P., Amici, A., Bellouin, N., Schmied, H. M., Hersbach, H., Buontempo, C., and Cagnazzo, C.: WFDE5 over land merged with ERA5 over the ocean (W5E5 v2.0), https://doi.org/10.48364/ISIMIP.342217, 2021.

Lange, S., Mengel, M., Treu, S., and Büchner, M.: ISIMIP3a atmospheric climate input data, https://doi.org/10.48364/ISIMIP.982724.2, 2023.

Lehner, B. and Döll, P.: Development and validation of a global database of lakes, reservoirs and wetlands, J. Hydrol., 296, 1–22, https://doi.org/10.1016/j.jhydrol.2004.03.028, data available at https://www.worldwildlife.org/pages/global-lakes-and-wetlands-database, accessed 2018-08-15, 2004.

Lehner, B., Liermann, C. R., Revenga, C., Vörösmarty, C., Fekete, B., Crouzet, P., Döll, P., Endejan, M., Frenken, K., and Magome, J.: High-resolution mapping of the world's reservoirs and dams for sustainable river-flow management, Frontiers in Ecology and the Environment, 9, 494–502, 2011.

Lutz, F., Herzfeld, T., Heinke, J., Rolinski, S., Schaphoff, S., von Bloh, W., Stoorvogel, J. J., and Müller, C.: Simulating the effect of tillage practices with the global ecosystem model LPJmL (version 5.0-tillage), Geosci. Model Dev., 12, 2419–2440, https://doi.org/10.5194/gmd-12-2419-2019, 2019.

Mengel, M., Treu, S., Lange, S., and Frieler, K.: ATTRICI v1.1 – counterfactual climate for impact attribution, Geoscientific Model Development, 14, 5269–5284, https://doi.org/10.5194/gmd-14-5269-2021, 2021.

Meyerholt, J., Sickel, K., and Zaehle, S.: Ensemble projections elucidate effects of uncertainty in terrestrial nitrogen limitation on future carbon uptake, Global Change Biol., 26, 3978–3996, https://doi.org/10.1111/gcb.15114, 2020.

Minoli, S., Jägermeyr, J., Asseng, S., Urfels, A., and Müller, C.: Global crop yields can be lifted by timely adaptation of growing periods to climate change, Nat. Commun., 13, 7079, https://doi.org/10.1038/s41467-022-34411-5, 2022.

Monfreda, C., Ramankutty, N., and Foley, J. a.: Farming the planet: 2. Geographic distribution of crop areas, yields, physiological types, and net primary production in the year 2000, Global Biogeochem. Cycles, 22, GB1022, https://doi.org/10.1029/2007GB002947, data available from http://www.earthstat.org/, accessed 2018-10-30, 2008.

Mueller, N.: Crop-specific global fertilizer application rates from "Closing yield gaps through nutrient and water management", Version 1, Zenodo, https://doi.org/10.5281/zenodo.5260732, accessed 2022-03-08, 2012.

Mueller, N. D., Gerber, J. S., Johnston, M., Ray, D. K., Ramankutty, N., and Foley, J. A.: Closing yield gaps through nutrient and water management, Nature, 490, 254–257, https://doi.org/10.1038/nature11420, 2012.

https://doi.org/10.5194/egusphere-2026-4549
Preprint. Discussion started: 28 September 2026

Müller, C., Elliott, J., Chryssanthacopoulos, J., Arneth, A., Balkovic, J., Ciais, P., Deryng, D., Folberth, C., Glotter, M., Hoek, S., et al.: Global gridded crop model evaluation: benchmarking, skills, deficiencies and implications, Geoscientific Model Development, 10, 1403–1422, https://doi.org/10.5194/gmd-10-1403-2017, 2017.

Müller, C., Elliott, J., Kelly, D., Arneth, A., Balkovic, J., Ciais, P., Deryng, D., Folberth, C., Hoek, S., Izaurralde, R. C., et al.: The global gridded crop model intercomparison phase 1 simulation dataset, Scientific data, 6, 1–22, https://doi.org/10.1038/s41597-019-0023-8, 2019.

Ostberg, S., Müller, C., Heinke, J., and Schaphoff, S.: LandInG 1.0: a toolbox to derive input datasets for terrestrial ecosystem modelling at variable resolutions from heterogeneous sources, Geoscientific Model Development, 16, 3375–3406, https://doi.org/10.5194/gmd-16-3375-2023, 2023.

Peltoniemi, M. S., Duursma, R. A., and Medlyn, B. E.: Co-Optimal Distribution of Leaf Nitrogen and Hydraulic Conductance in Plant Canopies, 32, 510–519, https://doi.org/10.1093/treephys/tps023, 2012.

Portmann, F. T., Siebert, S., and Döll, P.: MIRCA2000-Global monthly irrigated and rainfed crop areas around the year 2000: A new high-resolution data set for agricultural and hydrological modeling, Global Biogeochem. Cycles, 24, GB1011, https://doi.org/10.1029/2008GB003435, 2010a.

Portmann, F. T., Siebert, S., and Döll, P.: MIRCA2000, Version 1.1 [Data set], Zenodo, https://doi.org/10.5281/zenodo.7422506, accessed 2018-03-19, 2010b.

Porwollik, V., Rolinski, S., Heinke, J., von Bloh, W., Schaphoff, S., and Müller, C.: The role of cover crops for cropland soil carbon, nitrogen leaching, and agricultural yields – a global simulation study with LPJmL (V. 5.0-tillage-cc), Biogeosciences, 19, 957–977, https://doi.org/10.5194/bg-19-957-2022, 2022.

Rost, S., Gerten, D., Bondeau, A., Lucht, W., Rohwer, J., and Schaphoff, S.: Agricultural green and blue water consumption and its influence on the global water system, Water Resour. Res., 44, https://doi.org/10.1029/2007WR006331, 2008.

Schaphoff, S., Heyder, U., Ostberg, S., Gerten, D., Heinke, J., and Lucht, W.: Contribution of permafrost soils to the global carbon budget, Environ. Res. Lett., 8, 014 026, https://doi.org/10.1088/1748-9326/8/1/014026, 2013.

Schaphoff, S., Forkel, M., Müller, C., Knauer, J., von Bloh, W., Gerten, D., Jägermeyr, J., Lucht, W., Rammig, A., Thonicke, K., and Waha, K.: LPJmL4 – a dynamic global vegetation model with managed land – Part 2: Model evaluation, Geosci. Model Dev., 11, 1377–1403, https://doi.org/10.5194/gmd-11-1377-2018, 2018a.

Schaphoff, S., von Bloh, W., Rammig, A., Thonicke, K., Biemans, H., Forkel, M., Gerten, D., Heinke, J., Jägermeyr, J., Knauer, J., Langerwisch, F., Lucht, W., Müller, C., Rolinski, S., and Waha, K.: LPJmL4 – a dynamic global vegetation model with managed land – Part 1: Model description, Geosci. Model Dev., 11, 1343–1375, https://doi.org/10.5194/gmd-11-1343-2018, 2018b.

Schaphoff, S., von Bloh, W., Rammig, A., Thonicke, K., Biemans, H., Forkel, M., Gerten, D., Heinke, J., Jägermeyr, J., Langerwisch, F., Lucht, W., Rolinski, S., Waha, K., Ostberg, S., Wirth, S. B., Fader, M., Drüke, M., Jans, Y., Lutz, F., Herzfeld, T., Minoli, S., Porwollik, V., Stehfest, E., de Waal, L., Beringer (Erbrecht), T., Rost (Jachner), S., Gumpenberger, M., Heyder, U., Werner, C., Braun, J., Breier, J., Stenzel, F., Mathesius, S., Hemmen, M., Billing, M., Oberhagemann, L., Sakschewski, B., and Müller, C.: LPJmL: central open-source github repository of LPJmL at PIK, https://doi.org/10.5281/zenodo.17911585, 2025.

Schaphoff, S., Hötten, D., Müller, C., Gerten, D., Ostberg, S., and von Bloh, W.: Implementing methane dynamics into the LPJmL6 model, EGUsphere, 2026, 1–61, https://doi.org/10.5194/egusphere-2025-6210, 2026.

Scheer, C., Fuchs, K., Pelster, D. E., and Butterbach-Bahl, K.: Estimating Global Terrestrial Denitrification from Measured N2O:(N2O + N2) Product Ratios, Current Opinion in Environmental Sustainability, 47, 72–80, https://doi.org/10.1016/j.cosust.2020.07.005, 2020.

https://doi.org/10.5194/egusphere-2026-4549
Preprint. Discussion started: 28 September 2026

Sitch, S., Smith, B., Prentice, I. C., Arneth, A., Bondeau, A., Cramer, W., Kaplan, J. O., Levis, S., Lucht, W., Sykes, M. T., Thonicke, K., and Venevsky, S.: Evaluation of ecosystem dynamics, plant geography and terrestrial carbon cycling in the LPJ dynamic global vegetation model, Global Change Biol., 9, 161–185, https://doi.org/10.1046/j.1365-2486.2003.00569.x, 2003.

Smith, B., Wårlind, D., Arneth, A., Hickler, T., Leadley, P., Siltberg, J., and Zaehle, S.: Implications of incorporating N cycling and N limitations on primary production in an individual-based dynamic vegetation model, Biogeosciences, 11, 2027–2054, https://doi.org/10.5194/bg-11-2027-2014, 2014.

Sophia, G., Caldararu, S., Stocker, B. D., and Zaehle, S.: Leaf Habit Drives Leaf Nutrient Resorption Globally alongside Nutrient Availability and Climate, Biogeosciences, 21, 4169–4193, https://doi.org/10.5194/bg-21-4169-2024, 2024.

Sutton, M. A., Bleeker, A., Howard, C. M., Bekunda, M., Grizzetti, B., de Vries, W., van Grinsven, H. J. M., Abrol, Y. P., Adhya, T. K., Billen, G., Davidson, E. A., Datta, A., Diaz, R., Erisman, J. W., Liu, X. J., Oenema, O., Palm, C., Raghuram, N., Reis, S., Scholz, R. W., Sims, T., Westhoek, H., and Zhang, F. S.: Our Nutrient World: The Challenge to Produce More Food and Energy with Less Pollution, NERC/Centre for Ecology & Hydrology, Edinburgh, 2013.

Tarnocai, C., Canadell, J. G., Schuur, E. A. G., Kuhry, P., Mazhitova, G., and Zimov, S.: Soil organic carbon pools in the northern circumpolar permafrost region, Global Biogeochemical Cycles, 23, https://doi.org/https://doi.org/10.1029/2008GB003327, 2009.

Thornley, J. H. M.: A Transport-resistance Model of Forest Growth and Partitioning, Annals of Botany, 68, 211–226, https://doi.org/10.1093/oxfordjournals.aob.a088246, 1991.

Tian, H., Yang, J., Xu, R., Lu, C., Canadell, J. G., Davidson, E. A., Jackson, R. B., Arneth, A., Chang, J., Ciais, P., Gerber, S., Ito, A., Joos, F., Lienert, S., Messina, P., Olin, S., Pan, S., Peng, C., Saikawa, E., Thompson, R. L., Vuichard, N., Winiwarter, W., Zaehle, S., and Zhang, B.: Global Soil Nitrous Oxide Emissions since the Preindustrial Era Estimated by an Ensemble of Terrestrial Biosphere Models: Magnitude, Attribution, and Uncertainty, Glob. Change Biol., 25, 640–659, https://doi.org/10.1111/gcb.14514, 2019.

Tian, H., Xu, R., Canadell, J. G., Thompson, R. L., Winiwarter, W., Suntharalingam, P., Davidson, E. A., Ciais, P., Jackson, R. B., Janssens-Maenhout, G., Prather, M. J., Regnier, P., Pan, N., Pan, S., Peters, G. P., Shi, H., Tubiello, F. N., Zaehle, S., Zhou, F., Arneth, A., Battaglia, G., Berthet, S., Bopp, L., Bouwman, A. F., Buitenhuis, E. T., Chang, J., Chipperfield, M. P., Dangal, S. R. S., Dlugokencky, E., Elkins, J. W., Eyre, B. D., Fu, B., Hall, B., Ito, A., Joos, F., Krummel, P. B., Landolfi, A., Laruelle, G. G., Lauerwald, R., Li, W., Lienert, S., Maavara, T., MacLeod, M., Millet, D. B., Olin, S., Patra, P. K., Prinn, R. G., Raymond, P. A., Ruiz, D. J., van der Werf, G. R., Vuichard, N., Wang, J., Weiss, R. F., Wells, K. C., Wilson, C., Yang, J., and Yao, Y.: A Comprehensive Quantification of Global Nitrous Oxide Sources and Sinks, Nature, 586, 248–256, https://doi.org/10.1038/s41586-020-2780-0, 2020.

von Bloh, W., Schaphoff, S., Müller, C., Rolinski, S., Waha, K., and Zaehle, S.: Implementing the nitrogen cycle into the dynamic global vegetation, hydrology, and crop growth model LPJmL (version 5.0), Geosci. Model Dev., 11, 2789–2812, https://doi.org/10.5194/gmd-11-2789-2018, 2018.

Vörösmarty, C. J., Fekete, B. M., Meybeck, M., and Lammers, R. B.: Global system of rivers: Its role in organizing continental land mass and defining land-to-ocean linkages, Global Biogeochem. Cycles, 14, 599–621, https://doi.org/10.1029/1999GB900092, 2000.

Wang, H., Atkin, O. K., Keenan, T. F., Smith, N. G., Wright, I. J., Bloomfield, K. J., Kattge, J., Reich, P. B., and Prentice, I. C.: Acclimation of Leaf Respiration Consistent with Optimal Photosynthetic Capacity, Global Change Biology, 26, 2573–2583, https://doi.org/10.1111/gcb.14980, 2020.

Wirth, S. B., Braun, J., Heinke, J., Ostberg, S., Rolinski, S., Schaphoff, S., Stenzel, F., von Bloh, W., Taube, F., and Müller, C.: Biological nitrogen fixation of natural and agricultural vegetation simulated with LPJmL 5.7.9, Geosci. Model Dev., 17, 7889–7914, https://doi.org/10.5194/gmd-17-7889-2024, 2024.

https://doi.org/10.5194/egusphere-2026-4549
Preprint. Discussion started: 28 September 2026

Yu, T. and Zhuang, Q.: Modeling Biological Nitrogen Fixation in Global Natural Terrestrial Ecosystems, Biogeosciences, 17, 3643–3657, https://doi.org/10.5194/bg-17-3643-2020, 2020a.

Yu, T. and Zhuang, Q.: Modeling Biological Nitrogen Fixation in Global Natural Terrestrial Ecosystems, Biogeosciences, 17, 3643–3657, https://doi.org/10.5194/bg-17-3643-2020, 2020b.

Zaehle, S., Friend, A. D., Friedlingstein, P., Dentener, F., Peylin, P., and Schulz, M.: Carbon and Nitrogen Cycle Dynamics in the O-CN Land Surface Model: 2. Role of the Nitrogen Cycle in the Historical Terrestrial Carbon Balance, Glob. Biogeochem. Cycles, 24, https://doi.org/10.1029/2009GB003522, 2010.

Zhang, B., Tian, H., Lu, C., Dangal, S. R. S., Yang, J., and Pan, S.: Manure nitrogen production and application in cropland and rangeland during 1860–2014: A 5-minute gridded global data set for Earth system modeling, Earth Syst. Sci. Data Discuss., pp. 1–35, https://doi.org/10.5194/essd-2017-11, 2017.

Zhang, B., Tian, H., Lu, C., Dangal, S. R. S., Yang, J., and Pan, S.: Manure nitrogen production and application in cropland and rangeland during 1860 - 2014: A 5-minute gridded global data set for Earth system modeling, [Data set], PANGAEA, https://doi.org/10.1594/PANGAEA.871980, accessed 2022-05-04, 2017.